Załącznik nr. 3

Scientific Curriculum Vitae
(Autoreferat)

Methods of the Earth gravity field morphological analysis in relation to lithosphere structure

dr Lech Krysiński
Road and Bridge Research Institute
Pavement Diagnostic Division

Contents

1. FIRST AND LAST NAME

Lech Krysiński

2. DIPLOMAS AND SCIENTIFIC DEGREES, INCLUDING DATE OF AWARD AND NAME, LOCATION OF AWARDING INSTITUTION AND TITLE OF PHD DISSERTATION

- **Professional title of MSc** obtained in Physics, speciality: physics of lithosphere, Faculty of Physics, University of Warsaw 1991, title of MSc dissertation: *On the mathematical connections of planetary rotational deformations with Love's tidal problem for liquid planet* (L. Krysiński 1992);
- **PhD degree**, in Physics, awarded by Scientific Council of Faculty of Physics, University of Warsaw 1997, title of the PhD thesis: *Dynamical morphology of the Earth's magnetic field in the light of its evolution in period 1900-1995 and plurality of paleomagnetic observations*.

3. INFORMATION ON PREVIOUS AND CURRENT EMPOYMENT IN RESEARCH INSTITUTIONS

- 1992-1997, PhD studies, Faculty of Physics, University of Warsaw;
- 1997-2010, assistant professor (adjunct), Institute of Geophysics, Faculty of Physics, University of Warsaw, ul. Pasteura 7, 02-093 Warszawa;
- From 2010, assistant professor (adjunct), Pavement Diagnostic Division, Road and Bridge Research Institute, ul. Instytutowa 1, 03-302 Warsaw.

4. SCIENTIFIC ACHIEVEMENTS AS PER ART. 16 P. 2 LAW DATED ON 14 MARCH 2003 ON THE SCIENTIFIC DEGREES AND ON THE SCIENTIFIC TITLES AND ON THE DEGREES AND THE TITLES IN SCOPE OF ARTS (POLISH: DZ. U. 2016 R. POZ. 882 ZE ZM. W DZ. U. Z 2016 R. POZ. 1311.)

4.1 TITLE OF THE SCIENTIFIC ACHIEVEMENT

Methods of the Earth gravity field morphological analysis in relation to lithosphere structure

4.2 LIST OF PUBLICATIONS CONSTITUTING SCIENTIFIC ACHIEVEMENT

H1. Krysiński L., 2009. *Systematic Methodology for Velocity-dependent Gravity Modelling of Density Crustal Cross-Sections, using an Optimization Procedure*. Pure appl. geophys., 166, 375–408, doi: 10.1007/s00024-009-0445-x.

H2. Krysiński L., Wybraniec S. & Grad M., 2015. *Lithospheric density structure study by isostatic modelling of the European geoid*. Studia Geophysica et Geodaetica 2015 (2), 59, 212-252, DOI: 10.1007/s11200-014-1014-z.

H3. Krysiński L., Grad M. & Wybraniec S., 2009. *Searching for Regional Crustal Velocity-Density Relations with the Use of 2-D Gravity Modelling – Central Europe Case*. Pure appl. geophys., 166, 1913–1936, doi: 10.1007/s00024-009-0526-x.

H4. Krysiński L., Grad M., Mjelde R., Czuba W., Guterch A., 2013. *Seismic and density structure of the lithosphere-asthenosphere system along transect Knipovich Ridge-Spitsbergen-Barents Sea - geological and petrophysical implications*. Polish Polar Research, 34, 2, 111-138, doi: 10.2478/popore-2013-0011.

H5. Krysiński L., Grad M. & POLONAISE'97 Working Group, 2000. POLONAISE'97 - *Seismic and gravimetric modelling of the crustal structure in the Polish Basin*. Phys. Chem. Earth (A), 25 (4), 355-363, doi: 10.1016/S1464-1895(00)00057-0.

4.3 DISCUSSION OF THE SCIENTIFIC GOAL AND PRESENTATION OF THE OBTAINED RESULTS, INCLUDING DISCUSSION OF THE POSSIBLE APPLICATIONS

The anomalies of the earth gravity fields manifested are differences of observed gravity field from a reference model approximating the state of planetary hydrostatic equilibrium. Those anomalies are the result of the Earth internal structure complexity related to internal processes expressed in horizontal density changes. The most detailed and precise information about the internal Earth structure comes from seismic observation and research. Over time, the seismic results started to be used more and more effectively to explain the Earth gravity field shape. This activity became a crucial part of the Physics of the Earth gravity field. These comparisons have been conducted in different space scales from local (single rock massives; Puziewicz et al. 2012) and very local (single geological structures and technological objects), through regional (tectonic units expressed in crustal structure), up to continental and global scale (in which structural features of the lower mantle and Earth core manifest themselves). The basic research question is to determine how effectively the regional Earth gravity field shape can be modelled using the seismic data using some concepts of density attribution to seismic structures. Moreover, as a result of such modelling, suggestions about the density of some of these structures are put forward and consequently, these suggestions are important in pertrophysical considerations. Sometimes, the gravity modelling leads to suggestions about the structural model modifications, especially in the concept of the tectonic division of the area. In that way, the gravity modelling broadens our knowledge about the internal structure of the Earth.

The described cycle of papers gives an illustration to the methods of the lithosphere structure research of the European Plate in terms of the lithosphere density features through the gravity field shape modelling based on seismic results in regional (section 4.3.A) and continental scale (section 4.3.B). The referred efforts were to great extend methodological in its nature – their purpose was to formulate gravity modelling procedures used in a systematic way closely related to seismic data, enabling their numerical implementation and studying their mathematical properties with clear visualisation of the models' important features.

As the presentation of the reformulated methodology is very detailed and extensive, the most important results are underlined in the text of the appropriate chapters below.

4.3.A) Methodology of the velocity-dependent gravity modelling of the medium density distribution along deep seismic soundings profiles

Following the intensive development of refractive deep seismic soundings (Guterch i in. 2000, 1991, 1986), the new significant possibilities on commenting local and regional gravity field shape (Bielik i in. 2006, Grabowska i in. 2011, 1998) with the use of the crustal velocity sections were opened. The 2D seismic models along profiles (fig. 1) are particularly interesting because they provide the most detailed and precise imaging of the crustal structure at present, even if they do not give any insight into the structural change in the lateral direction. Information about the structure is contained in the layer system and P-velocity distribution of the seismic model. The most basic version of the gravimetric modelling consists in density attribution to each layer – the density is constant inside the given layer. Next, the layer density values are adjusted to match the gravity field of this density model to the observed gravity anomaly along the profile. In 2D approach it is assumed that the structure of the medium does not change in the direction perpendicular to the profile. This assumption can be adequate when the profile runs approximately perpendicularly to the crossed tectonic boundaries.

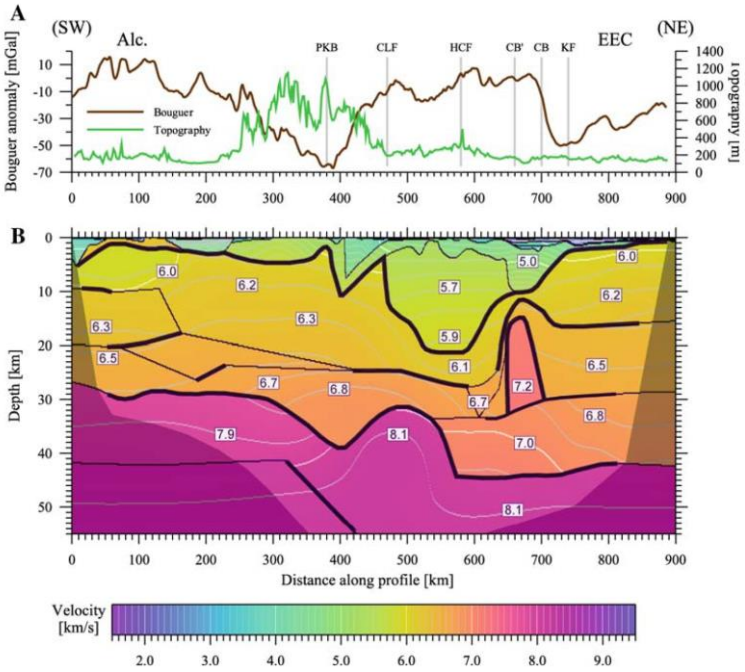

Figure 1. Input data for gravity modelling. **A)** Topography and gravity anomalies along the profile. **B)** Two-dimensional P-wave velocity model for CELEBRATION 2000 profile CEL01 obtained by forward ray tracing modelling (Środa et al. 2006). The black thick solid lines are elements of mid-crustal boundaries verified by reflected and/or refracted rays, and thin lines are iso-velocity contours in km·s^{-1}. Shaded areas at the bottom of the model and in both lower corners show parts of the model that are not constrained by refracted and reflected waves (no ray coverage).

Just the first experience with this task shows that matching the layer density set is not an easy task. It is caused by a very strong interdependence of density parameters (H5). In spite of the linear dependence of model field on density parameters, an attempt to define an inverse problem as a standard fitting procedure leads in practice to the defeat, as unrealistic values are attributed to the density parameters; this is a classical instability problem accompanying the adjustment of the large number of mutually interdependent parameters. Thus, in this procedure, limits for densities must be applied to each density value. Each limit value must be contained inside the acceptable value range appropriate to the given structural layer. Approximate estimations for acceptable values come from the long tradition of global Earth structure investigation. Moreover, the significant phenomenological interdependence between density of typical rocks (constituting the crust and the Earth mantle) and their wave velocity $\boldsymbol{v_p}$ (defined in the seismic section; fig. 2) is very helpful. The classical form of this interdependence seems to be influenced by the opinions related to the Precambrian cratonic crust and is opened to some doubts as to its adequacy in case of Phanerozoic areas (H3). Nevertheless, the existence and possibility of approximate parameterisation of the limits for acceptable density values through the velocity $\boldsymbol{v_p}$ is the key element of contemporary models of the crustal density structure based on modelling of the observed gravity field and the determined seismic structure.

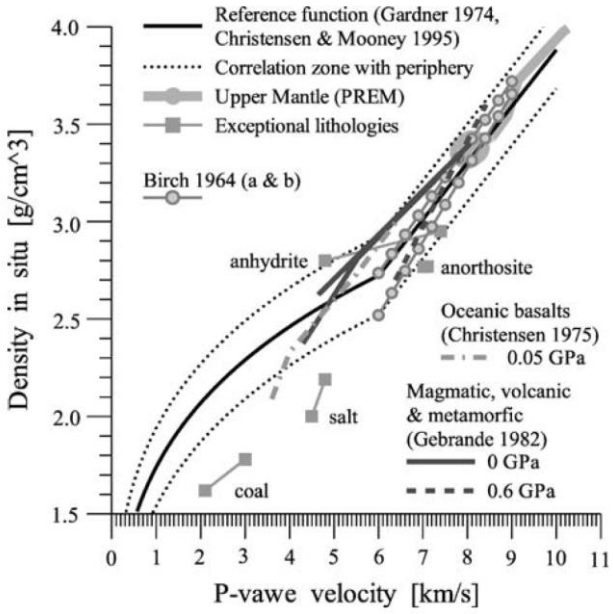

Figure 2. The definition of the reference function $\boldsymbol{\rho_{ref}(v)}$ (central solid line) describing the correlation between density and velocity for rocks constituting the crust and the uppermost mantle (model of the central velocity-density correlation zone). Some other models are presented in the background for comparison (H1).

The described procedure along with its difficulties was an impulse for the formulation of the gravimetric modelling procedure in the form of optimisation task, which after a numerical implementation would allow to answer the questions about existence of satisfactory solution for the density model and about stability of the matched density parameters in the case of a given density section successfully. The first attempts already showed (H5) that this approach is very promising, but new challenges of the problem appeared at the same time.

The importance of the structural information contained in the wave velocity spatial distribution. Attributing one density value to each layer based on the wave velocity (observed inside the layer) brings about immediate dilemmas. It is not obvious whether the density limits should be linked to the average velocity value or maybe linked separately to the minimum and maximum ones respectively (extending the allowed range with some tolerance). These deliberations lead to the supposition that spatial velocity changes inside a layer probably contain an interesting information about the spatial density changes, and in particular, about the horizontal changes generating reasonable gravity effect (H1). Thus, a need arose for the further development of numerical models of the density field that would parameterise density changes inside the given layer, so that after imposing limitations on the density model parameters, the limitation will be satisfied in every point of the seismic section. After long-term attempts, the numerically implementable solution satisfying these demands was adopted in the following form (H4, Krysiński i in. 2009):

$$\begin{aligned} \rho(x,z) &= \rho_{ref}(v(x,z)) + H_{K(x,z)}(v(x,z)) \\ -\Delta\rho &< H_{K(x,z)}(v(x,z)) < \Delta\rho \end{aligned} \quad . \qquad (1)$$

The function $\boldsymbol{\rho_{ref}}$ is the adopted reference density-velocity dependence (fig. 2), and the function $\boldsymbol{H_k(v)}$ locally correcting the reference value $\boldsymbol{\rho_{ref}(v(x,z))}$ is a piece-wise linear function (in particular cases, it can be linear or constant function) of the velocity argument and it has a separate form in every layer with its own parameters (fig. 3). The function $\boldsymbol{K(x,z)}$ gives the layer number, which the point of coordinates $\boldsymbol{(x,z)}$ belongs to. The layer system can be freely defined in reference to the seismic layers or independently from them. The values $\boldsymbol{h_i}$

of the piece-wise linear function $\boldsymbol{H_k}$ in its knot points $\boldsymbol{v_i}$ are the natural parameters defining the function $\boldsymbol{H_k}$ (fig. 3). Under this definition, it is enough to superimpose demand $\boldsymbol{-\Delta\rho < h_i < \Delta\rho}$ on every knot parameter to satisfy the density limitations (1) for the density model $\boldsymbol{\rho(x, z)}$ with density tolerance $\boldsymbol{\Delta\rho}$ in relation to the reference value $\boldsymbol{\rho_{ref}(v(x, z))}$ in every point $\boldsymbol{(x, z)}$ of the section. The gravity field of this density model depends linearly on the parameters $\boldsymbol{h_i}$. Thus, it is possible to implement the classical optimisation procedure with constraints in the form of limitations. It consists in the determination of model parameters values ($\boldsymbol{h_1}$, $\boldsymbol{h_2}$,…, $\boldsymbol{h_N}$), which minimize difference in $\mathbf{L^2}$ norm between the gravity field of the density model and the gravity field observed along the profile while keeping the limitations ($\boldsymbol{-\Delta\rho < h_i < \Delta\rho;\ i} = 1, 2,\ldots, \boldsymbol{N}$) for parameters $\boldsymbol{h_i}$. The set of all density parameter vectors ($\boldsymbol{h_1}$, $\boldsymbol{h_2}$,…, $\boldsymbol{h_N}$) allowed by the limitations as a subset of $\mathbf{R^N}$ is convex here. Thus, the solution of the task is unambiguous in the sense that all local solutions (local minima) correspond to the same minimal value of the residue and they constitute a convex set (H5). Inambiguity and possibility of precise numerical determination of the minimal residue value $\boldsymbol{R_{min}}$ (being a measure of the model mismatch) are the key properties of this method, because they allow to analyse the residue behaviour for the determination of the optimal model, for example.

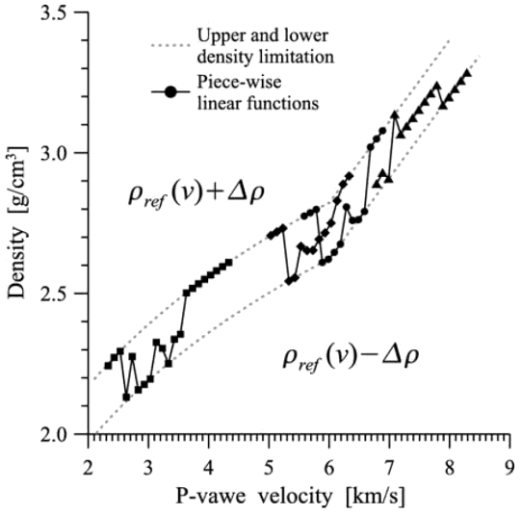

Figure 3. The definition of the general velocity-dependent density distribution model $\boldsymbol{\rho_{ref}(v)} + \boldsymbol{H_k(v)}$, as a sum of the reference relation $\boldsymbol{\rho_{ref}(v)}$ and a piece-wise linear functions $\boldsymbol{H_k(v)}$ for an artificial case of four layers ($\boldsymbol{k} = 1, 2, 3, 4$); (typical velocity section consists of a few tens of layers). Knot points for each layer are represented by different symbols: squares, diamonds, circles and triangles. Each two functions can have different shapes in the common part of their velocity ranges and the corresponding curves can even cross each other because their constructions are independent. Note that dashed lines limit the interpolating functions.

The numerical implementation of such a task allows to answer the question whether the velocity distribution inside the layers bears an interesting information about the density distribution. When the model density distribution is very flexible in each layer (having a form of piece-wise linear function with numerous knots) the task is a numerical challenge, as the total number of the model parameters could be counted in hundreds. After twelve years of developing the *Gravity Modelling System* the effective calculations became possible to answer the aforementioned question. In fact, the contemporary seismic models contain significant information about spatial density distribution contained in the distribution of the P-wave velocity inside layers (H1).

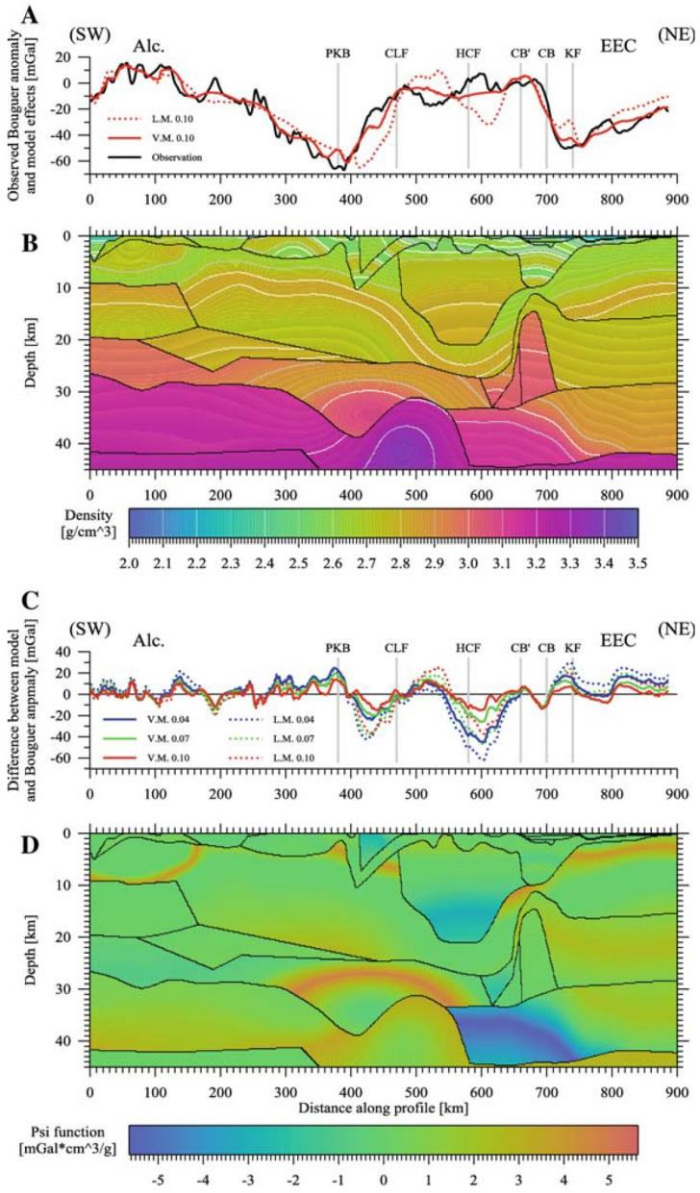

Figure 4. Results of the velocity-layer-dependent modelling for the profile CEL01. **A)** Comparison of the observed Bouguer anomaly and results of the model (***z*** = 80 km and $\Delta\rho$ = 0.1 g/cm^3). Black solid line represents observed Bouguer anomaly and red lines represent model values: solid line for velocity dependent modelling (V.M.) and dashed line for layer-dependent modelling (L.M.). **B)** The density cross-section (for velocity resolution 0.1 km/s) obtained for ***z*** = 80 km and $\Delta\rho$ = 0.1 g/cm^3. Black lines are layer boundaries postulated in seismic model. **C)** Stability test of zero points: Comparison of the spatial distribution of residuals (difference between gravity field of the model and observation), for two methods of modelling, and for three values of the density tolerance $\Delta\rho$ = 0.04, 0.07 and 0.1 g/cm^3 (***z*** = 80 km). The amplitude of residuals increases if $\Delta\rho$ decreases. **D)** Function $\psi(x, z)$ characterizing influence of local density overestimation or underestimation (forced by superimposed density limitation) on matching misfit: Red areas correspond to overestimated density and blue correspond to underestimated density.

Nevertheless, the model density distribution determined as a result of the modelling assuming the standard form of limitation (1) for densities has a visible disadvantage when large flexibility of the correcting function is allowed (dense knot set). In this case, the density distribution inside many layers shows non-realistic alternating variations of value (rys 3 i 4B),

which reflect the mentioned instability in matching a large number of parameters, but sometimes it seems to be a result of lacking or improper layer division into regional segments, as well (rys. 4B i D). This problem was resolved later in a subsequent modification of the optimisation task definition and it resulted in several methods imaging the intensity of systematic tendency of the density in the given part of section to be adjusted below or above the reference value (fig. 4D; H1). These methods are a very useful tool in local and regional petrological and tectonic analyses (H4), because they give a stable illustration of local density $\boldsymbol{\rho}(\boldsymbol{x}, \boldsymbol{z})$ anomalies in relation to the reference value $\boldsymbol{\rho_{ref}}(\boldsymbol{v}(\boldsymbol{x}, \boldsymbol{z}))$ suggested for the local seismic velocity $\boldsymbol{v}(\boldsymbol{x}, \boldsymbol{z})$. The experience coming from observations of the described instability allowed to formulate criteria for reasonable limitations of the number of density parameters. It turns out that attributing more than one or two parameters to one layer is usually not necessary (H3, H4) with the exception of very thick layers like the whole crust.

Significance of isostasy in lithosphere-asthenosphere system. When analysing and modelling Bouguer anomaly distribution in regional scale (hundreds of kilometres), one can expect significant influence of *isostasy* i.e. the tendency of the lithosphere-asthenosphere system toward reaching buoyancy equilibrium. In modelling practice this supposition means that the differences of mass per length postulated in vertical columns of the density model inside the section window along the profile should be compensated below the window in downward continuation of columns. Then, in these columns extended down to some sublithospheric level the density per profile length unit does not depend on the distance. The compensation results in weakening of the model gravity field changes in large space scales.

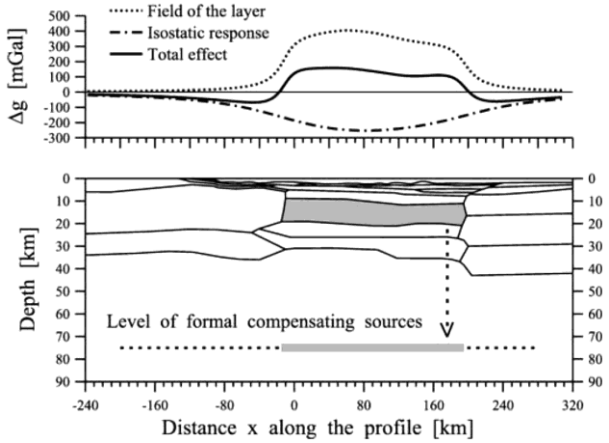

Figure 5. Simulation of the subcrustal isostatic response using the concept of formal compensating sources positioned on one level. All mass above the maximal depth of the well-documented seismic structure (e.g. 45 km) is projected with an opposite sign on one deeper level of depth $\boldsymbol{z}$. Mass distribution and resulting field corresponding to one homogeneous layer (marked in grey) is depicted as an example (H1, H5).

The insight into crustal structure provided by refractive deep seismic soundings sections usually reaches depths of several kilometres below the Moho. Thus, the principle of isostasy is used for the reconstruction of the mass distribution in the lithosphere-asthenosphere system below the Moho. The details of this distribution have much less influence on the gravity field shape observed on the surface than the crustal masses, because the subcrustal masses are very deep. Thus, in the present approach *the model of formal compensating sources* (H5, H1) was applied. In this model all compensating masses are put on one level of depth $\boldsymbol{z}$ (below Moho), and they are defined as anti-projection of the all masses postulated by the density model in the section window (fig. 5). In this model the additional gravity field produced by the

compensating sources depends linearly on density parameters h_i of the model, and the inclusion of this effect does not cause difficulties in the procedure definition and its numerical implementation. The depth z should be understood as a characteristic depth of a subcrustal zone of horizontal fluctuations of the compensating density sources, but the real spatial distribution (especially in a vertical direction) has a large ambiguity and it remains an open question in this approach.

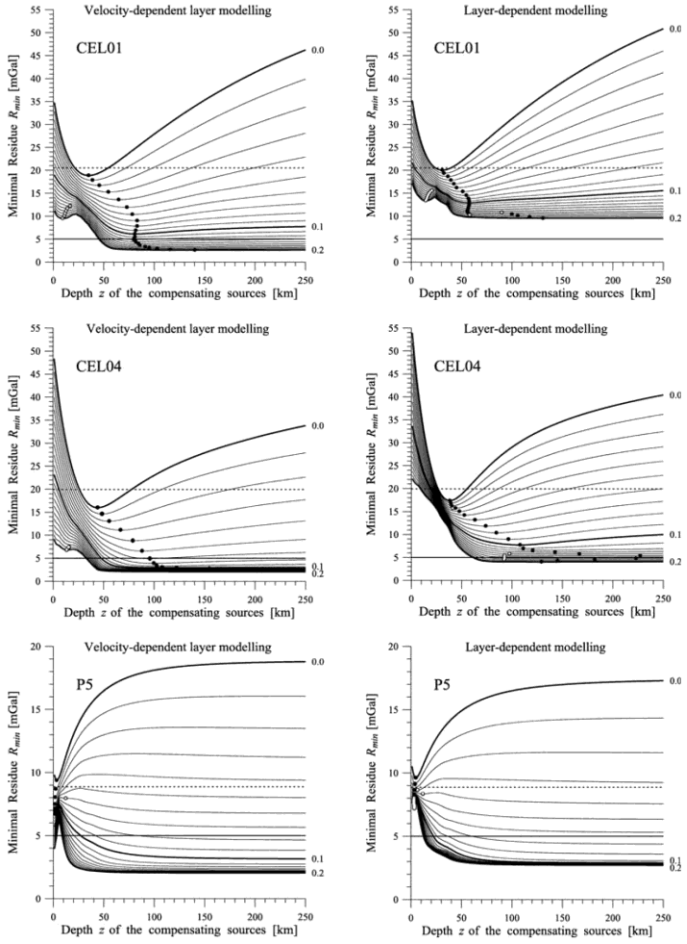

Figure 6. Residual diagrams for the considered seismic profile CEL01 and for two other profiles (CEL04 and P5; Środa et al. 2006, Czuba et al. 2001) drawn for a comparison (the two modelling methods for each profile). The minimal residue R_{min} (root mean-square of residuals of gravity model matching) obtained by optimisation of the density parameters is depicted as a function of depth z of the level of formal compensating sources. Each curve corresponds to a different value of the density tolerance $\Delta\rho$. The $\Delta\rho$ starts from 0 and increases up to 0.2 g·cm^{-3} with a step of 0.01 g·cm^{-3}. The curves corresponding to $\Delta\rho$ = 0, 0.1, and 0.2 g·cm^{-3} are marked by thick lines. A solid circle marks the main minimum for a given curve and other local minima are drawn as open circles. The dashed horizontal lines mark dispersion δf of the Bouguer anomaly variation for the profile. The solid horizontal line marks 5 mGal, i.e., the level of acceptable residue value.

In this research, the question as to the significant presence of isostasy was treated as a hypothesis under investigation. The results of the modelling show clearly that in fact, the influence of isostasy is visible (H5, H1). It is manifested as minima of the matching residue R_{min} (fig. 6) considered as a function of the depth z of compensating sources level, when the density tolerance $\Delta\rho$ remains constant and it is close to its value 0.1 g/cm^3 expected for rocks,

which constitute crust. These minima occur at subcrustal positions, usually several tens of kilometres below the Moho. Nevertheless, the difference between the residue of such optimal model and the residue of a counterpart model without compensation (limit of $z \rightarrow \infty$) is not large. It means that the models without compensation could have similar efficiency in the field approximation, but they probably underestimate large-scale horizontal contrasts. The described proofs of isostasy are not observed in cases of very short profiles and profiles running along axis and boundaries of tectonic structures. This observation shows that the 2D gravity modelling is sensitive to the degree in which the demand of the 2D symmetry is fulfilled by the medium structure and the profile course. Under these demands the tectonic realms are correctly reflected in the modelling. It also confirms the supposition that isostasy is a lithosphere's feature present in a large space scales of hundreds kilometres.

Divisional analysis of seismic section. The residual differences between observed Bouguer anomaly and its model have many possible reasons (fig 4A and 4C; H1). Among the most important ones are the breaking of the assumption of the 2D medium structure and the course of the profile not perpendicular to boundaries of the assumed 2D structure. In particular, the local structures frequently do not fit the general 2D architecture of the region, even where the last one is present at all. The universality of the reference density-velocity relation also raises many doubts (H3). Even if all these exemplifying doubts were to be moderated, the adequacy of the layer-velocity seismic models (fig. 1) as a representation of regional medium structure does not make it a less essential problem. Frequently, a necessity to modify the layer system or to polemicise with suggested velocity values in some places arises. Usually, some parts of the section do not provide enough adequate and documented structure's image (fig. 1). In the central parts of profiles, the layer system and vertical velocity distribution usually have reliable bases, while the sections not always have enough horizontal resolution to localize deep (approximately vertical) boundaries between tectonic units, which in particular, are manifested in the morphology of potential fields. Especially disputable is a continuation of uniform petrophysical identity (reflecting the genesis of tectonic units) of very long seismic layers, stretching for distances of many hundreds of kilometres crossing through tectonic units of a very varied genesis (fig. 1). Thus, a need for modification of the initial models arises, leading to matching improvement (decrease of the residue $\boldsymbol{R_{min}}$) and regionalisation (division into regional segments) of the crust along the profile. In the light of the constructed methodology of gravity modelling, the modifying of the seismic section is a controversial step, because the initial layer-velocity model is the crucial canvas stabilizing the density distribution about some realms of the medium, which are measurable and clearly connected with density. An exception can be made with respect to the aforementioned argumentation and in principle the modifications can only have a form of divisions by approximately vertical boundary lines. The implementation of the ***divisional procedure*** was inspired by discussions about a very interesting case of Świętokrzyski Fault (Grabowska et al. 2011), which has no noticeable expression in the wave velocity $\boldsymbol{v_p}$ field (Środa et al. 2006), but it is a distinctive tectonic and lithological boundary, and it has clear manifestation in the gravity field (e.g. figs 4A, 5C; distance 560 km). Usually, the modifying of the layer system is performed by an arbitrary decision, at the distance of significant gravity mismatch and succeeding corrections leading to improvement of gravity matching, while the goal of the divisional procedure was a partial objectivisation of this interpretation practice to allow visualisation of the divisional steps showing their necessity. The present approach was preceded by the pioneering trial of numerical realisation of the task in numerical form (Pabisiak 2005), which showed at practical level that these basic assumptions make sense.

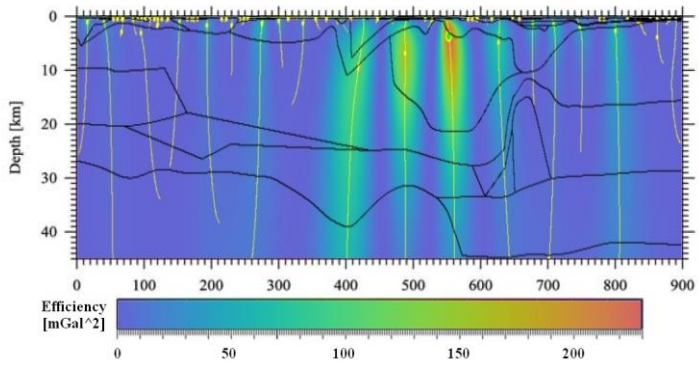

Figure 7. Similarity function (efficiency) calculated from the residual field for the initial density modelling. The high values correspond to places where division by vertical boundary would be particularly effective in residuals reduction (Krysiński et al. 2009).

Next, after several years of tests the experimental divisional procedure based on the described methods of velocity-dependent modelling was created. The procedure interprets the residual gravity field (the difference between the model and observed Bouguer anomaly) resulting in a freely chosen variant of the modelling, showing the most optimal place for division. The section showing a *potential efficiency* (so called *similarity function*) in improvement of matching derived from a division, made at the given distance and depth, gives the visualisation of the place choice (fig. 7). The division is made by a vertical line in the place where the efficiency function has the maximal value, but in the area not occupied by division defined earlier. The maximum points to the layer to be divided and this layer is replaced by two new layers having separate, independent density parameters for succeeding gravity modelling. The defining of succeeding divisions continues until the residue of matching $\boldsymbol{R_{min}}$ decrease below an assumed earlier threshold e.g. $\boldsymbol{R_{kryt}} = 2$ mGal. In this procedure a decreased density tolerance value $\boldsymbol{\Delta\rho}$ is preferred e.g. about $0.05 g \cdot cm^{-3}$ assuming that areas of anomalous deviations of density from the reference value will finally be framed during the course of the procedure.

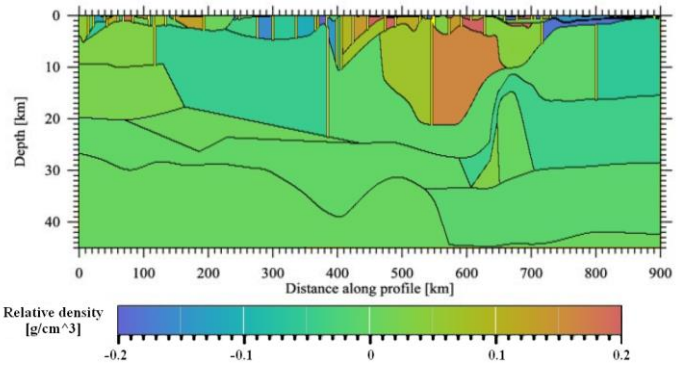

Figure 8. The relative density (density deviations related to the reference values) a section with postulated layer divisions (yellow lines) after the correction of their positions (Krysiński et al. 2009).

After defining of the divisions system the sequential verification is started. It consists in a removal of one division and repeat postulation of its position by the designation of a new optimal place. In that way the positions of all divisions are being verified sequentially, and the entire cycle is repeated several times. As a result, the procedure provides a section with suggested divisions system, which can be interpreted using aforementioned methods. In

particular, the new section shows clearly the spatial arrangement of the density anomalies (fig. 8; H1, H4).

In spite of extensive efforts the divisional procedure is not a clearly defined mathematical problem, as opposed to the modelling methods themselves. The results of this procedure depend on the assumed density tolerance value and the final residue value threshold. The doctrine of the layer definitions is also problematic, because the layer cannot be partly divided, but must be divided across its whole thickness. In this matter, when searching for major tectonic boundaries, it would be strongly advised to divide the whole crust (across its whole thickness) after the earlier simplification of the crustal layer system. On account of the ambiguity of the divisional method, the wider family of divided models should be taken into account in succeeding interpretations, including different initial definitions of the layer system and using different values for the process parameters ($\boldsymbol{R_{kryt}}$ i $\boldsymbol{\Delta\rho}$). The tracking of the process could be valuable, because it allows for the identification of more stable elements in regionalisation of the density field. The particular attention should be put on the divisional efficiency function of the initial model (fig. 7), which usually bears a clear and stable intention, showing the position and quite often some inclination of cardinal horizontal density contrasts. The method has an interesting application as an efficient tool of the tectonic regionalisation of the profile and identification of the anomalous density structures (H4).

The problem of the reference density-velocity relation. As mentioned above, the reference velocity-density relation $\boldsymbol{\rho_{ref}(v)}$ (fig. 2) plays a very significant role in the described velocity-dependent gravity modelling. The supposition that density has quasi-functional interdependence with velocity $\boldsymbol{v_p}$ for rocks which typically form the Earth's crust and mantle, which can be transferred onto average properties of large rock massives, is the fundamental assumption within contemporary practice of gravity modelling, based on structural results of the refraction seismics. The tradition of investigating this relation has several tens of years and it is documented by a wide body of literature (H1). This activity consists mainly of laboratory measurements, the density $\boldsymbol{\rho}$ and velocity $\boldsymbol{v_p}$ of rocks (especially in high pressure conditions). But also some less stable opinions as to the usefulness of different reference relations in gravity modelling were formed. The postulation of the reference density-velocity relation on the base of laboratory measurements is called sometimes as petrological modelling.

The modelling method described earlier was extensively tested on a dozens of profiles passing through the area of Poland. Thus some systematic tendencies of the density adjustment near upper or lower limit of the allowed reference zone were observed (Krysiński 2006). In this situation an idea of searching for the reference relation using the gravity modelling appeared (H3). The principles of this procedure are similar to the modelling, but the task is defined in another way. In this case the reference relation (in simple form defined by several parameters only) is being searched for, to match (minimising the residue) the observed Bouguer anomaly to the model field; obtained as a result of the conversion of velocity into density (using the reference relation) followed by its transformation into a model gravity field. The attempts to complete such a task, even on very long but single transects, give unstable results. Thus it was decided to perform this modelling on four transects altogether (fig. 9).

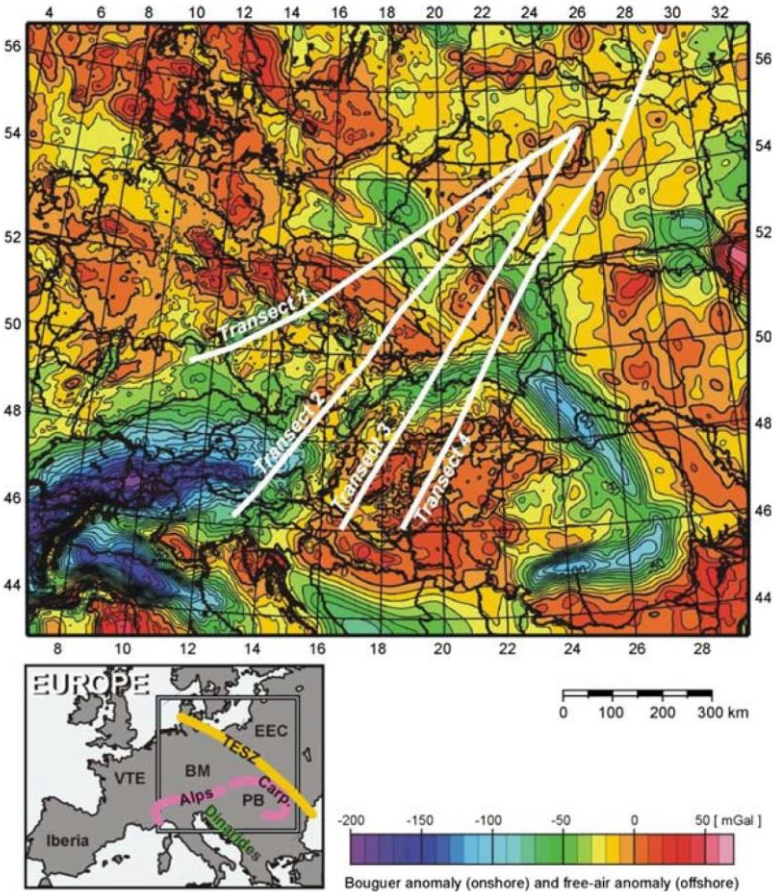

Figure 9. Location of four seismic transects plotted on the gravity anomaly map of Central Europe (Wybraniec 1999). The rectangle in the insert shows the study area; BM-Bohemian Massif; Carp.-Carpathians; EEC-East-European Craton (Baltica); PB-Pannonian Basin; TESZ-Trans-European Suture Zone; VTE-Variscan terranes of Europe.

The result of the modelling (fig. 10) would seem to confirm the traditional opinion as to the density value in the uppermost mantle just below the crust (fig. 10 lower left), but the shape of this reference relation in the crystalline crust has much weaker dependence on velocity than it is postulated in the classical models (fig. 2). The analysis of the distribution of the subcrustal compensating density sources also needs some larger thought. The attempt to attribute a realistic spatial arrangement to these masses leads to a vision of a low-density layer in the uppermost mantle underlying the area of Phanerozoic Europe (H3, fig. 11). These results gave a reason to study the difference between the two provinces Praecambrian and Phanerozoic while one more deeply. The model field matching to the observed anomalies though acceptable is not a very good one, which happens to be a typical feature for general models with a small parameters number. It attracts attention that, the particularly large mismatch is observed in a wide transitional zone between the two provinces (H3). This effect reflects not only the distinct contrast of their petrophysical properties, but also it reflects large dilemmas in determination of the boundary position between them. When these two areas are being modelled separately (omitting the transitional zone), they seem to be essentially different in features expressed by the density-velocity relation (fig. 10, lower right). The relation $\rho_{ref}(v)$ in the Easteuropen Craton is close to the classical one, while in Phanerozoic geoprovince the crystalline crust seems to have its density very weakly dependent on velocity (what suggests plagioclase-rich composition) and the uppermost mantle of a surprisingly low density 3.15-3.2 g·cm^{-3} which could be a hallmark of extensive Tertiary rift processes.

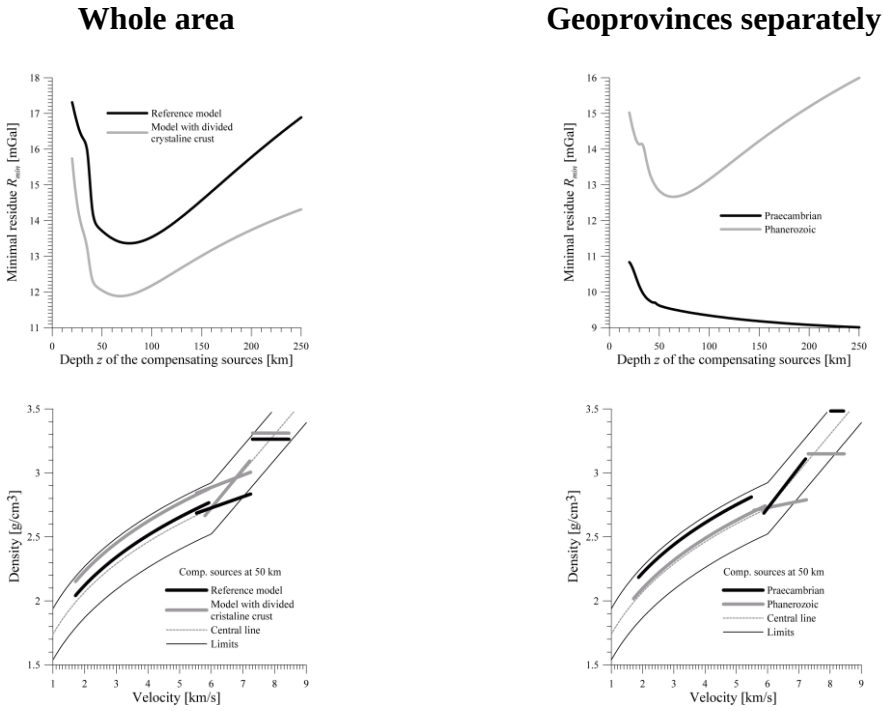

Figure 10. The dependence of the minimal residue R_{min} on the depth z of compensating sources (residual diagrams; top) and examples of the resulting velocity-density relations (for nearly optimal, extremely shallow depth z = 50 km and giving the largest mantle density; bottom), obtained in the fitting procedure applied to the four profiles treated together. On the left throughout the entire area and on the right for the two provinces, which were modelled separately.

After a longer analysis it turns out that the classical opinions on the density-velocity relation (fig.2) in the crystalline crust staunchly prefer the Praecambrian cratonic type of lithology and these opinions neglect a possibility of significant participation of plagioclases in the composition of the lower parts of the crust, what can be potentially possible feature of them in Phanerozoic units.

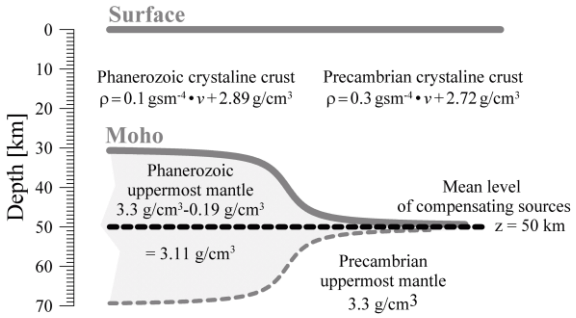

Figure 11. Schematic reinterpretation of the compensating masses model assuming the optimal shallow position of compensating sources (z = 50 km).

4.3.B) Study of the lower lithosphere density structure by geoid modelling in a continental scale

The modelling of the geoid shape in the area of the European Plate was undertaken to test the relation of the field shape with topography and morphology of the Moho surface (Grad et al. 2009) in the continental scale (fig. 12). The density stratification of the lower lithosphere including a discussion of the lithosphere-asthenosphere transition nature in terms of gravity response was the central subject matter of this study. The geoid shape is an alternative representation of the gravity field anomalies. As opposed to anomalies of the gravity field this representation lessens the small-scale horizontal variations emphasising shape components of regional and continental dimensions. For this reason the geoid shape is considered to be a much better manifestation of the gravity influence of deep density anomalies situated in lower lithosphere, the aesthenosphere and in the deeper Earth's mantle including the lower mantle.

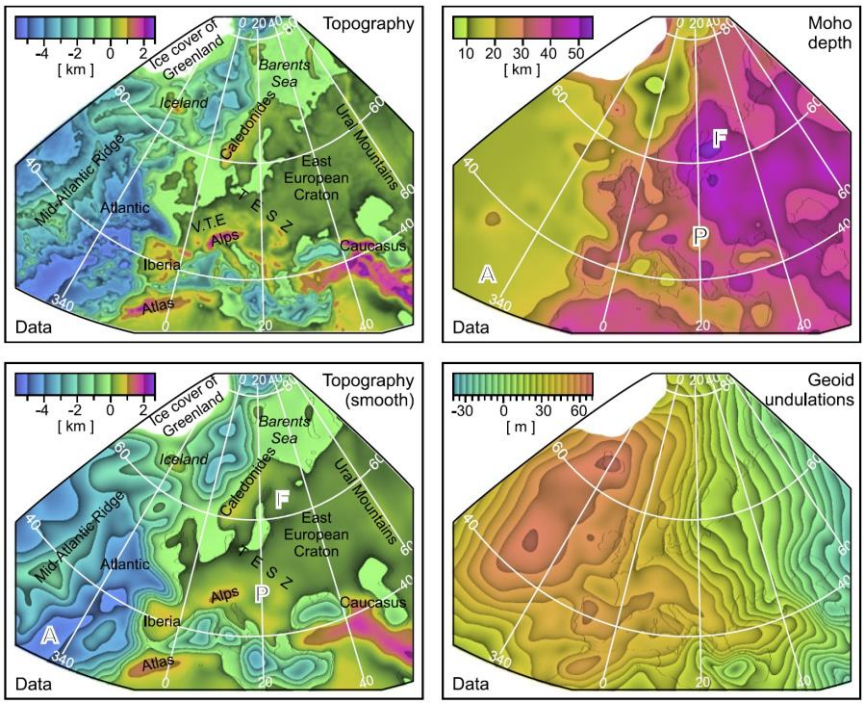

Figure 12. Input data for the European Plate, which were used in the geoid modelling (H2): topography/bathymetry (Becker et al. 2009), smoothed Moho depth (Grad et al. 2009), smoothed topography/bathymetry and smoothed geoid undulations (Pavlis et al. 2008) - with optimal smoothing scale 120 km. The Abyssal Atlantic Plain, Fennoscandian and Pannonian areas are marked by A, F and P, respectively.

Constructing of the lithospheric density model distribution in the continental scale. Density model of lithospheric column is postulated in the following form:

$$\rho_p^{mod}(z) = \rho_p^{ini}(z) + \rho_p^{comp}(z), \qquad (2)$$

where the initial distribution $\boldsymbol{\rho_p^{ini}}(z)$ correspond to a column consisting of mantle, crust and optionally water layer of thickness given by the input data ($\boldsymbol{z_p^{Moho}}$, $\boldsymbol{z_p^{Topo}}$ in the given point $\boldsymbol{p}$) with attributed some standard densities $\boldsymbol{\rho^a}$, $\boldsymbol{\rho^c}$, $\boldsymbol{\rho^w}$ respectively, while the superimposed compensating correction $\boldsymbol{\rho_p^{comp}}(\boldsymbol{z})$ has a form of a linear function of the depth $\boldsymbol{z}$, down to the depth $\boldsymbol{z_p^{Lith}}$, where it reaches the value of zero and deeper it remains nil. The two models of the compensating distribution were considered (fig. 13). The first one called the *Constant Contrast Model* (*CCM*) assumes a constant value $\boldsymbol{\beta}$ of the compensating correction $\boldsymbol{\rho_p^{comp}}$ in the roof of the lithosphere in the entire modelled area: $\boldsymbol{\rho_p^{comp}}(\boldsymbol{z_p^{Topo}}) = \boldsymbol{\beta}$. The second one is

named *Constant Gradient Model* (*CGM*) and it assumes in the entire modelling area a constant value γ of the gradient of correcting density distribution: $-d\rho_p^{comp}(z)/dz = \gamma$. The essence of the correcting density ρ_p^{comp} is to make the buoyancy compensation of the lithosphere laying on relatively plastic aesthenosphere resulted from its thermal regime. Thus the model density distribution fulfils the condition of isostatic equilibrium:

$$\int_{-\infty}^{+\infty} [\rho_p^{mod}(z) - \rho^{Ref}(z)]\, dz = 0, \qquad (3)$$

expressing an assumption that the weight of the column per surface unit is constant on the entire area i.e. it does not change between points $\boldsymbol{p}$ of the modelling area.
In the notation applied here the integral over the entire infinite range of the depth $\boldsymbol{z}$ has a symbolic meaning and represents integral over the range starting from some deep formal level below entire lithosphere and ending on some formal level over the topographic surface, i.e. is the integral over the entire interesting depth range. As a reference column usually the lithosphere of the axial zone of the oceanic ridges is used, which according to common opinions has a structure known with the least uncertainty or at least this structure gives rise to relatively not many fundamental controversies. The deviatoric load σ_p of the lower lithosphere by the initial crustal density column $\rho_p^{ini}(\boldsymbol{z})$:

$$\sigma_p = \int_{-\infty}^{+\infty} \rho_p^{ini}(z)\, dz - \int_{-\infty}^{+\infty} \rho^{Ref}(z)\, dz \qquad (4)$$

under the assumption of isostatic equilibrium is compensated by the load related to the superimposed correcting distribution $\rho_p^{comp}(\boldsymbol{z})$, which in oceanic area is an expression of the ocean floor cooling process, while in continental areas it could reflect the petrophysical differences between the regions as well.

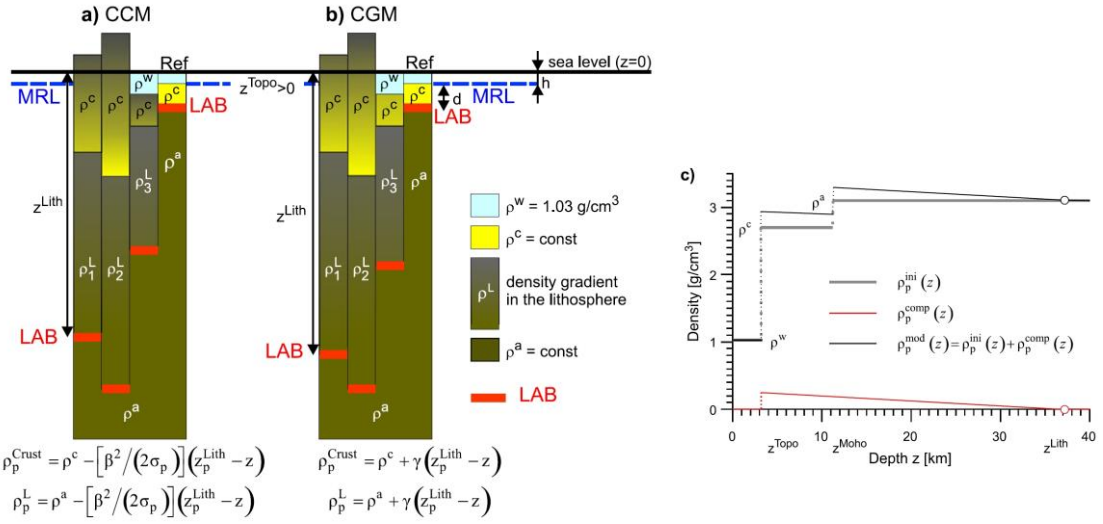

Figure 13. Schematic notation for the lithospheric models, discussed in the geoid modelling (H2), for the compensating density distribution: **a)** constant contrast model (CCM), **b)** constant gradient model (CGM). The models are composed of crust (with density stratification ρ_p^{Crust}) and lithospheric mantle (with density stratification $\rho^{L}{}_p$); seawater layer and asthenosphere have densities ρ^w and ρ^a, respectively. The elevation is described by z^{Topo} both for topography ($z^{Topo} < 0$) and bathymetry ($z^{Topo} > 0$); z^{Moho} is a Moho depth, z^{Lith} is a LAB depth (lithosphere-asthenosphere boundary). Abbreviation Ref is a reference column of lithosphere and MRL is an average mid-oceanic ridge level. In each case formulas for density in the crust and lithosphere are shown (ρ^{Crust} and ρ^{L} , respectively; see text for other explanations). **c)** An example of the model density distribution $\rho_p^{mod}(\boldsymbol{z})$ of oceanic type, and its parts: initial distribution $\rho_p^{ini}(\boldsymbol{z})$ and compensation $\rho_p^{comp}(\boldsymbol{z})$.

The calculating of the geoid in infinite flat layer approximation. In the geoid modelling the practice of the flat layer approximation is commonly used. It assumes the local lithosphere layer structure to be a flat horizontal infinite plate containing flat-parallel density stratification simulating the entire local system topography-lithosphere-asthenosphere. The tradition of this approximation use strengthened in its first fruitful applications to modelling of the oceanic ridges (Turcotte i Harris 1984). The perturbation of the potential $\boldsymbol{V}$ on the plate surface under this approximation has the following form:

$$\delta V_p = 2\pi G \int_{-\infty}^{+\infty} [\rho_p^{mod}(z) - \rho^{Ref}(z)] \cdot z \cdot dz \ . \tag{5}$$

The corresponding undulation is expressed as follows:

$$u_p^{lith} = \frac{-\delta V_p}{g} = -2\pi G \frac{m_p^{ini} + m_p^{comp} - m^{Ref}}{g}, \text{ where} \tag{6}$$

$$m_p^{ini} = \int_{-\infty}^{+\infty} \rho_p^{ini}(z) \cdot z \, dz, \quad m_p^{comp} = \int_{-\infty}^{+\infty} \rho_p^{comp}(z) \cdot z \, dz, \quad m_p^{Ref} = \int_{-\infty}^{+\infty} \rho_p^{Ref}(z) \cdot z \, dz \tag{7}$$

The geoid model is a sum of the model lithospheric undulation $\boldsymbol{u_p^{lith}}$ and the buffer polynomial $\boldsymbol{w_p}$ of variables $\boldsymbol{x}$, $\boldsymbol{y}$ parametrising the modelling area:

$$u_p^{mod} = w_p + u_p^{lith}, \quad w_p = \sum_{i=0}^{K} \sum_{j=0}^{i} \mu_{i,j} x_p^i y_p^{i-j}. \tag{8}$$

The simulation of the field of a very deep sublithospheric sources is the objective of the polynomial. The modelling task consists in matching the model undulation $\boldsymbol{u_p^{mod}}$ to the observed one:

$$u_p^{obs} \approx u_p^{mod}, \tag{9}$$

by adjusting the values of parameters $\boldsymbol{\gamma}$ or $\boldsymbol{\beta}$ and $\boldsymbol{\rho^c}$, $\boldsymbol{\rho^a}$ and coefficients $\boldsymbol{\mu_{i,j}}$ of the buffer polynomial.

It can be shown by using simple calculations and examples, why this a little surprising by its simplicity formula (5) has large effectiveness as the field approximation. The formula shows that the influence of the lithosphere density stratification on the gravity field potential is almost local. The essence of paradoxical loss of far gravity influence by the lithospheric sources is situated in a superimposed condition of isostatic equilibrium (3). Thus the elementary sources observed in the distance in regional-scale become dipolar sources loosing the far influence. The small plate thickness in relation to the Earth's radius and in relation to the scale of horizontal plate structure changes is a condition of the validity of this approximation. The second condition is a little problematic and it causes so that the geoid must be modelled using the smoothed input data.

The formula (5) has another important result also. One can notice that the influence of the lithospheric density stratification on the geoid shape (6) generally does not depend on the details of the density vertical distribution, but it depends on its moment only (7). Thus, many possible (and frequently considered in the literature) forms of stratification are mutually equivalent on account of their gravity effect observed in regional shape of the geoid. This observation allow for the understanding and comment on the large divergences in opinions as to the depth of formal boundary between lithosphere and asthenosphere (LAB, Lithosphere-Asthenosphere Boundary) occurring between different disciplines investigating this set of problems in terms of very different methods (seismic, gravimetric, thermal, petrophysical, magnetotelluric,…). Thanks to this observation and the modelling results described below, it becomes clear why the level of the formal compensating sources (fig. 5) usually has a very shallow position (fig. 6) of several tens of kilometres below Moho. The characteristic thickness of the lithosphere in this extremely agglomerated model is one third of the linear

model thickness Δ_{lith}. Thus, the dominating horizontal compensating density contrasts are situated in the upper part of the lower lithosphere.

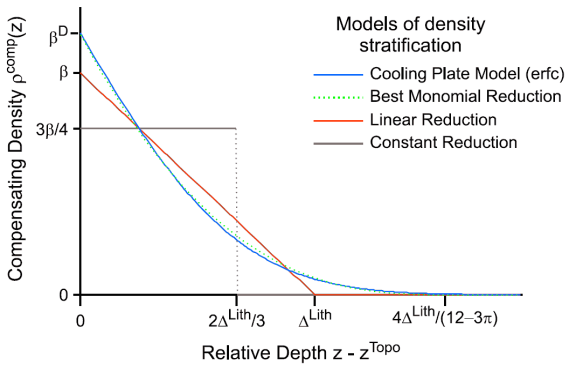

Figure 14. Density-depth relations (H2) used in the different variants of constant contrast model (CCM)/cooling plate model (CPM); $\boldsymbol{\beta}$ - density amplitude in equivalent linear reduction (ELR) exemplified by constant contrast model (CCM), $\boldsymbol{\beta^D}$ - density amplitude in cooling plate model (CPM), $\boldsymbol{\Delta^{Lith}}$ - conventional thickness of the lithosphere in terms of ELR.

In the cooling plate model this effect is obvious, while it is not always taken into account in the dialogue between disciplines investigating manifestations of the blurred foot part of the lithosphere and other disciplines approximating lower lithosphere by homogeneous layer, for instance. As an optimal compromise between views of different methods one can recommend the thickness $\boldsymbol{\Delta^{Lith}}$ of the linear model for a conventional definition of the lithosphere thickness; it would be treated then as Equivalent Liner Reduction (ELR; recalculation in to a linear model). But the identification of the physical nature in the different approaches and the determination of recalculation rules for the lithosphere characteristic parameters between them is much more important than the convention choice.

The decomposition of the geoid shape into the lithospheric part and the part corresponding to deep sublithospheric sources. Modelling of the lithosphere influence on the geoid shape in large regional or continental space-scales demands to take into account the presence of the field of sources much deeper than the density structure of the lithosphere-asthenosphere system, and they are situated in the sublithospheric upper mantle and in the lower mantle. Their influence is hardly visible in a local scale, where it is expressed as a constant background in undulation distribution. In a large regional scale the background has a form of a distinctive trend. But in a continental scale this background is a basic component of the modelled geoid shape. With respect to its very deep sources, this background has much more smooth shape than the part corresponding to the lithospheric density structure and this distinction is a basis of separation methods of these components. In the performed modelling the high-pass filtration or arbitrary definition of the sublithospheric part were given up to add *buffering polynomial* $\boldsymbol{w_p}$ (of the two cartographic coordinates $\boldsymbol{x}$, $\boldsymbol{y}$) to the model of lithospheric undulation (8). The coefficients $\boldsymbol{\mu_{i,j}}$ of this polynomial are being adjusted numerically in the fitting procedure together with density parameters of the model when on parameters $\boldsymbol{\rho^c}$, $\boldsymbol{\rho^a}$ limitations expressing current opinions as to their acceptable values (fig. 15) were superimposed, while parameters $\boldsymbol{\beta}$, $\boldsymbol{\gamma}$ and coefficients $\boldsymbol{\mu_{i,j}}$ were adjusted without limits. Thanks to this elastic approach to the simulation of the sublithospheric part there is a hope that the procedure would not load the determination of large-scale component of the lithospheric part by the field of deep origin. In this methodology the choice of the degree $\boldsymbol{K}$ of the buffer polynomial (8) is a critical issue. In this approach a novel idea of optimal degree determination was applied which consist in investigation of the degree influence on reduction

of the matching residue. The use of the polynomial has an obvious analogy to the high-pass filtration. Thus one can make a comparison of the polynomial use results to the results of the bottom cut of the harmonic series describing the global field shape EGM2008 (Pavlis i in., 2008), which was used as a source of input undulation data. The power spectrum of the global model illustrates the amplitude relations between the both components (lithospheric and sublithospheric ones) that it is possible to precise the criterion of optimal decomposition in the two filtration methods (H2).

The characterization of lithospheric density stratification in geoprovinces of the European Plate. The geoid modelling using the described method allows to estimate the characteristic values of the density stratification parameters $\boldsymbol{\beta}$ or $\boldsymbol{\gamma}$, because the residue of matching has a clear global minimum (fig. 15) in the range of expected values. These results give a motivation for the use of optimal values, but first of all they constitute a proof for correct construction of the modelling procedure, which has some novel filtration solutions demanding for not quite obvious calibration (buffering polynomial and initial smoothing of the input data).

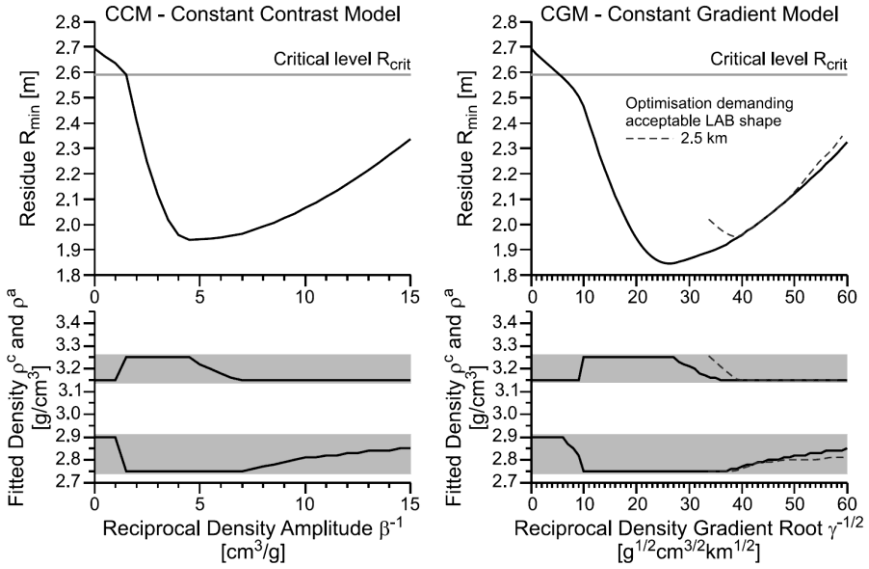

Figure 15. Estimation of the optimal lithospheric density parameters $\boldsymbol{\beta}$, $\boldsymbol{\gamma}$ using residual diagrams for concepts of isostatic compensation (H2): constant contrast model (left; CCM) and constant gradient model (right; CGM).

The estimations of the final (optimal) values of the parameters characterising the density stratification of the lithosphere depend visibly on the smoothing scale applied during preparation of the input data. This effect is a result of the assumed flat layer approximation with infinite plate that is, which neglects horizontal changes of the lithosphere structure near the point of the field observation (i.e. determination of the geoid undulation). Meanwhile, the input data for the modelling reflect also the structural changes occurring between small regions. These changes of the structure have influence on the potential value not only locally, but also in the vicinity of radius comparable the double characteristic depth of compensation sources. In particular, this approximation leads to systematic underestimation of the calculated undulation near its local extremes. It causes a systematic shift of the determined optimal stratification parameters in the modelling procedure. As the smoothing of the initial data moderates this effect – referring the calculation to regional average values the geoid and geometrical characteristics of the crust – it can be assumed that that the results corresponding

to larger values of the smoothing scale (e.g. the above-mentioned characteristic values) are more adequate characterization of the lithosphere of the given geoprovince (fig. 16)

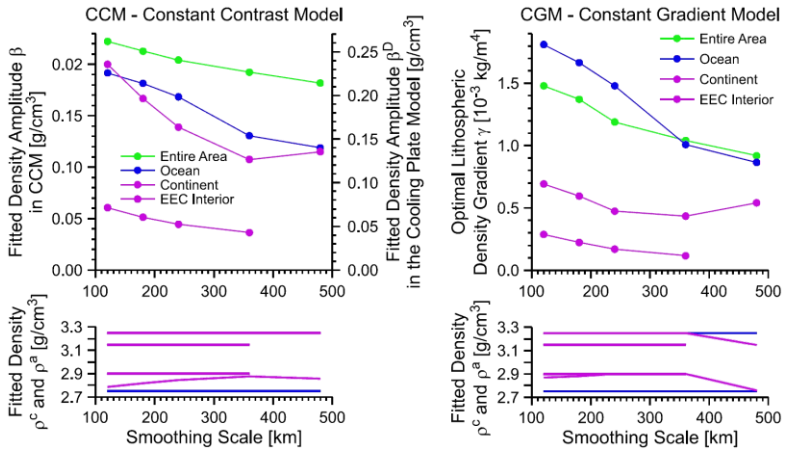

Figure 16. Calculated optimal parameters in modelling for constant contrast model (counterpart of the cooling plate model) (left) and constant gradient model (right) i.e. the two concepts of isostasy, as functions of the input data smoothing scale (H2). The value of the smoothing scale about 400-500 km would give a reasonable parameters estimation. Density curves for the entire area (green) are usually hidden behind oceanic curves (blue).

The results of the CCM model assuming the constant roof correcting density contrast, in the case of the oceanic area have a visible accordance with cooling plate model commonly accepted as an adequate, basic description of the ocean floor thermal evolution. The model of constant lithospheric gradient of the correction density CGM should be applied to some continental areas. But first of all it should be considered in the case of geoprovinces having as uniform as possible age and genetic characteristics to estimate their lithospheric density stratification. In the presented research the entire area was modelled, but also oceanic area, entire continental area and the interior of the Easteuropean Craton as a separate geoprovinces.

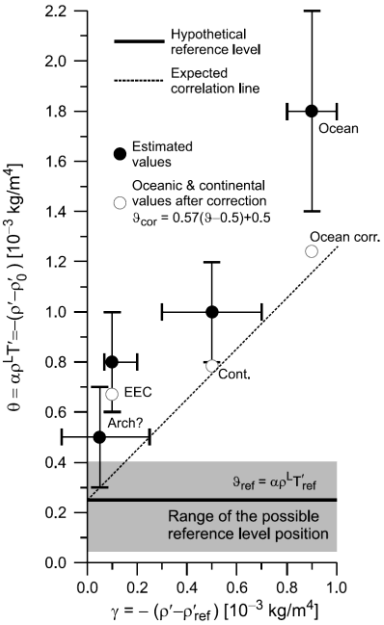

Figure 17. Interdependence between compensating density gradient γ (constant gradient model) and thermal estimation of the temperature part of the shallow density gradient θ observed in geo-provinces of the investigated area (H2).

The obtained estimations of the lithospheric density gradient shows a visible interdependence with the typical values of the subcrustal heat flow referred in the literature for the individual geoprovinces (fig. 17). The shape of this interdependence seems to reflect correctly the degree of the thermal evolution, which is essentially different in each of these provinces. Discussion of this interdependence is one of the most interesting results of this modelling.

The example of the geoid shape modelling (fig. 18a) provides also its decomposition into sublithospheric part (fig. 18e) and anomalies of the lithospheric origin (fig. 18c or alternative estimation resulting from the observed geoid fig. 18d). They give also visualisation of the anomalous crustal load of the mantle (fig. 18b). These maps are a wide inspiration to tectonic and genetic considerations for the entire area of the investigation (H2). The local residues, i.e. the differences between geoid model and its observation are usually less than 5 meters, and larger ones can indicate more the inadequacy of the crust model than the lithosphere deviations from isostatic equilibrium (fig. 18f).

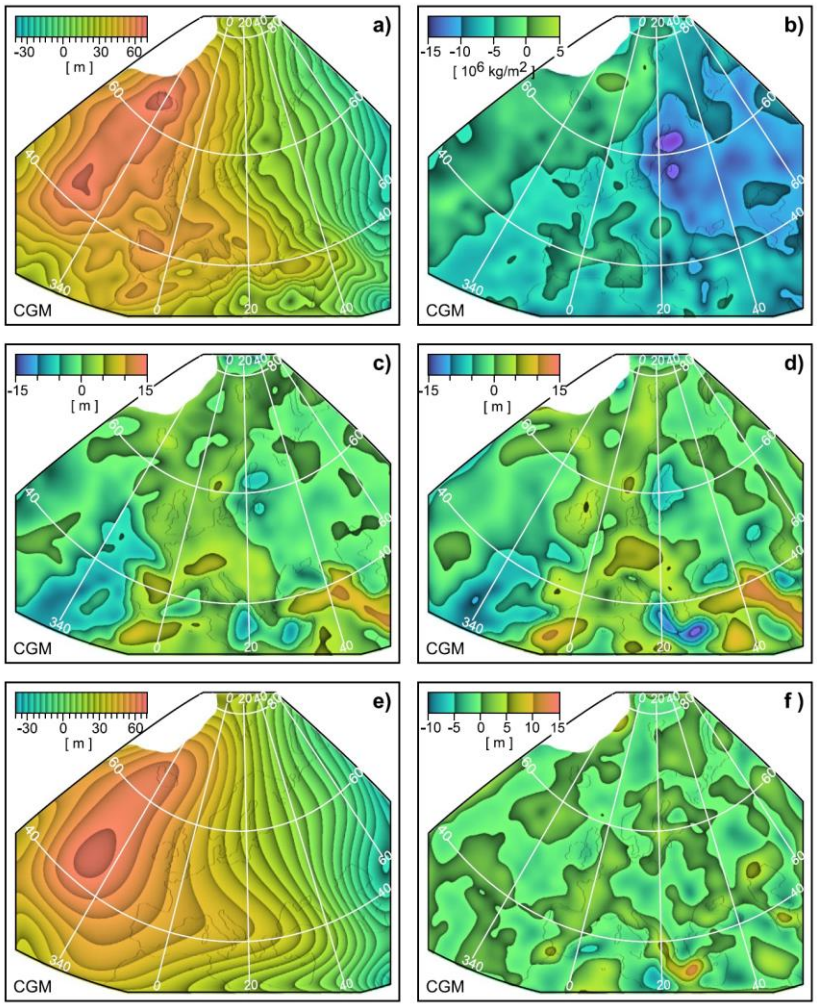

Figure 18. Example of resulting optimal model (smoothing scale of input data 120 km; H2), constant gradient model (CGM) of isostasy: **a)** model of geoid undulations; **b)** deviatoric load; **c)** model of the lithospheric undulations; **d)** separated lithospheric undulations (observed undulations after subtraction of the sublithospheric part); **e)** sublithospheric undulations; **f)** residuals.

The distribution of the lithosphere thickness below the European plate. The described modelling provides maps of the attributed depth $z_p^{Lith} = z_p^{Topo} + \Delta_p^{Lith}$ of the formal foot of the lithosphere (fig. 19). With respect to the severe discordance between the continental and the

oceanic area the example map was obtained by sewing together the results of the CCM model well fitting to the oceanic area, and CGM model which better describes realities of the continental lithosphere of more advanced thermal evolution and rich in crustal heat sources. This example shows the capability of the presented concept to commenting on the lithosphere thickness problem and in making agreement between opinions coming from different research disciplines. This is some suggestion for stabilization of the spatial interpolation of the lithosphere thickness data. The example of the model (fig. 19) should not be treated as the final result of this geoid modelling. This concept can be improved upon by the introduction of several important aspects influencing the isostatic equilibrium like the heat generation, thermal age characterising the degree of thermal evolution, and petrophysical differences between the geoprovinces, if these properties will be successfully described or parameterised in the future.

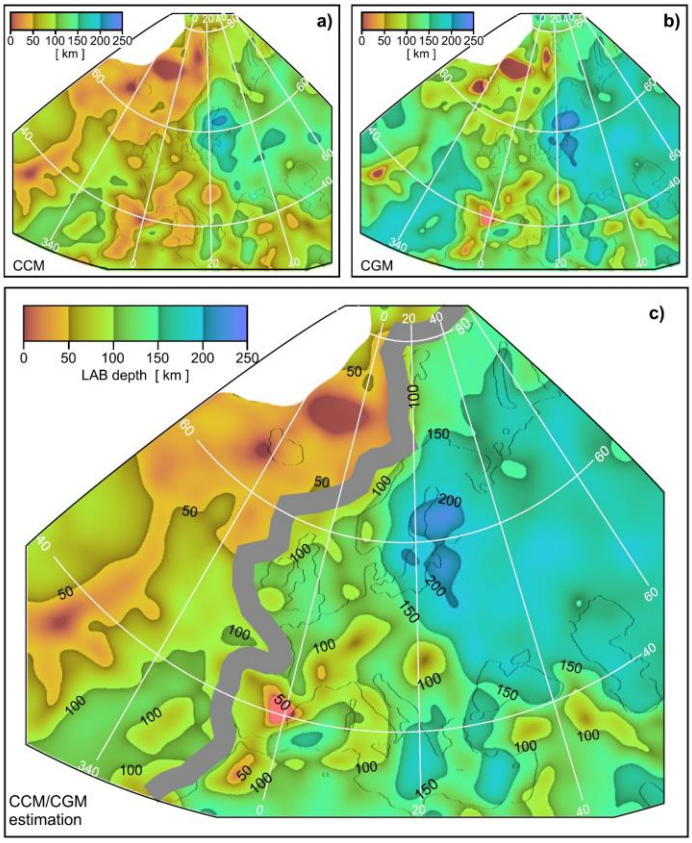

Figure 19. Lithosphere-asthenosphere boundary (LAB) depth (H2) for **a)** the constant contrast model (CCM) and **b)** constant gradient model (CGM) of isostasy using corrected values of parameters β or γ and densities optimised respectively for the oceanic area (CCM) or continent (CGM, optimisation constrained by accordance of LAB depth in Pannonia and Fennoscandia). **c)** Combination of LAB using the oceanic part from CCM and continental part from CGM, and the thick grey line indicates the continent-ocean transition (COT).

5. DISCUSSION OF OTHER SCIENTIFIC ACHIEVEMENTS

5.A) Global dynamical morphology of the Earth magnetic field

The goal of this research (Krysiński 1997, 1996) was to make as wide as possible review of the observations documenting the global properties of the Earth's magnetic field shape and its temporal behaviour, which would give the bases to formulate opinions about the process keeping up the field. The numerical investigation of the global field models collection given in the DGRF convention and covering XX century time range, was a particular part of this research.

A) The statistics of the leading periods

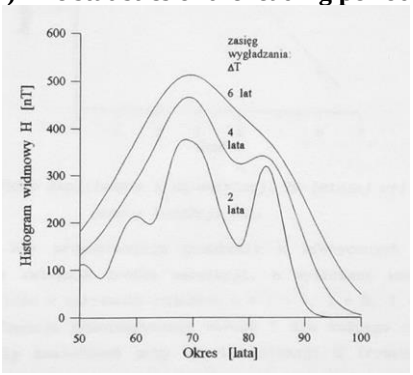

B) The total residue and amplitude

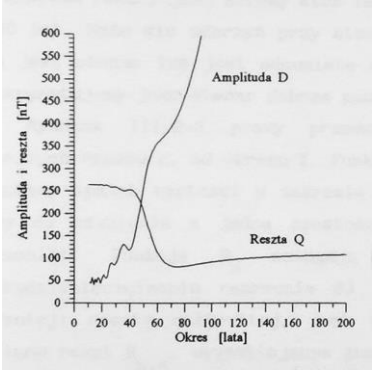

C) The total residues of the particular orders

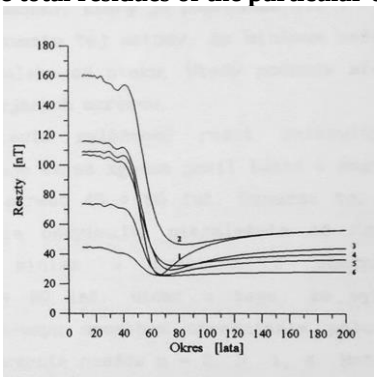

D) The amplitude spectrum

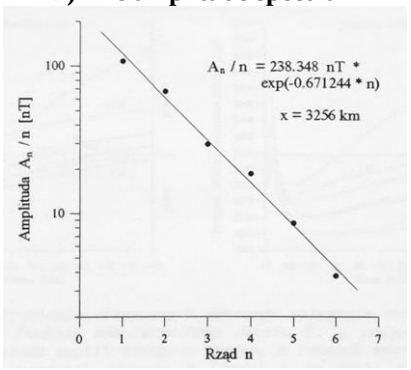

Figure 20. Results of investigation of *about 70-years oscillation* of the Earth's magnetic field in the XX-century, described by global models (DGRF 1900-1995). Optimal periods and amplitudes were being determined by a matching sinusoid with polynomial trend of second degree to each coefficient $g_{n,m}$ and $h_{n,m}$ of the field expansion series ($n \leq 6$). **A)** Spectral histogram illustrating root mean square amplitude of the field fluctuations (component ***Z***, Earth surface) in particular bands of the period; smoothed histogram (smoothing scale ΔT) of optimal periods for particular coefficients, weighted properly by their amplitudes. **B)** Determination of the fluctuation optimal period in this observation range by matching models to coefficients assuming a common period; ***D*** – total amplitude, ***Q*** – total residue. **C)** Determination of the optimal periods for particular degrees ***n*** of the expansion series, by common matching of models to coefficients of ***n***-th degree. **D)** Amplitude spectrum A_n/n of the 70-years oscillation in the semi-logarithmic diagram; this normalization gives for dipole source linear dependence of Log(A_n/n) on ***n***, which has inclination that characterizes in simple way the radius of the sphere containing the source.

In principle, these models are the best source at present allowing for global investigation of the properties of the field shape fluctuations in the several tens of years' period bands (fig. 20). The longest periods of this band provisionally called as *60-years* or *70-years oscillation* were the main subject of this research. In this working name occurs a tendency toward elongation of the name period following the elongation of the time span of the precise, continuous and global observations of the field. As a matter of fact this oscillation is not a regular oscillation with well-determined period, but it is a pseudo-periodic behaviour of the field representing the high-frequency edge of the *secular variation* available for the surface observations (rys. 20A). One can suppose straight out that this spectrum does not favour (in amplitude) specific frequencies, but its particular ranges have some typical amplitudes and some other characteristics like the depths of the sources position (fig. 20C). As a result of the spectral analysis it was successfully established that the characteristic level of the formal dipole sources of the 70-years fluctuation is situated about 200 km below core-mantle boundary (CMB, fig. 20D). In the light of the contemporary opinions this fluctuation should be associated first of all with the instable, non-stationary behaviour of the convection process in the outer core. The radial component of this oscillation transformed downward to the core-mantle boundary shows presence of many not very extensive areas of a well determined phase gradient (in the observation time span) which allow for further discussion of the hypothetical conditioning of the MHD process near the CMB (400-km-thick layer). In this research, the analogical analyses of the field behaviour for other bands of fluctuation period (20-years, 40-years, hundreds –years and thousands-years) were performed, but these oscillations have not yielded such good observation bases such as the described 70-years one.

A lot of attention was dedicated to properties analysis of the *main cycle* and of closely related phenomenon of the *field inversion* (*reversal*). In particular, the conception of interpreting of some systematic features in the course of inversions observed in the Upper Tertiary via its rock records in paleomagnetic results was presented. These reversal course features may reflect uneven heat transfer from the core to mantle at CMB surface (fig. 21). This idea is based on the notion that the large-scale magnetic flux density on the core surface determines the main field shape on the Earth's surface. The large-scale features of the field observed at present show that the core magnetic flux has got several widespread anomalies of very slow evolution of their total magnetic flux in relation to their shape changes. This behaviour can be associated with the current ideas about magnetohydrodynamical outer core convection, the thermal conditioning of this process and with the probable style of the large-scale flow. This conception leads to opinions about the nature and the general features of the anomalies evolution, giving a method of description of the global field shape evolution in millennial time-scales. Later the conception was supplemented by the method of description the specific wondering tracks of the Virtual Geomagnetic Pole (VGP) during inversion.

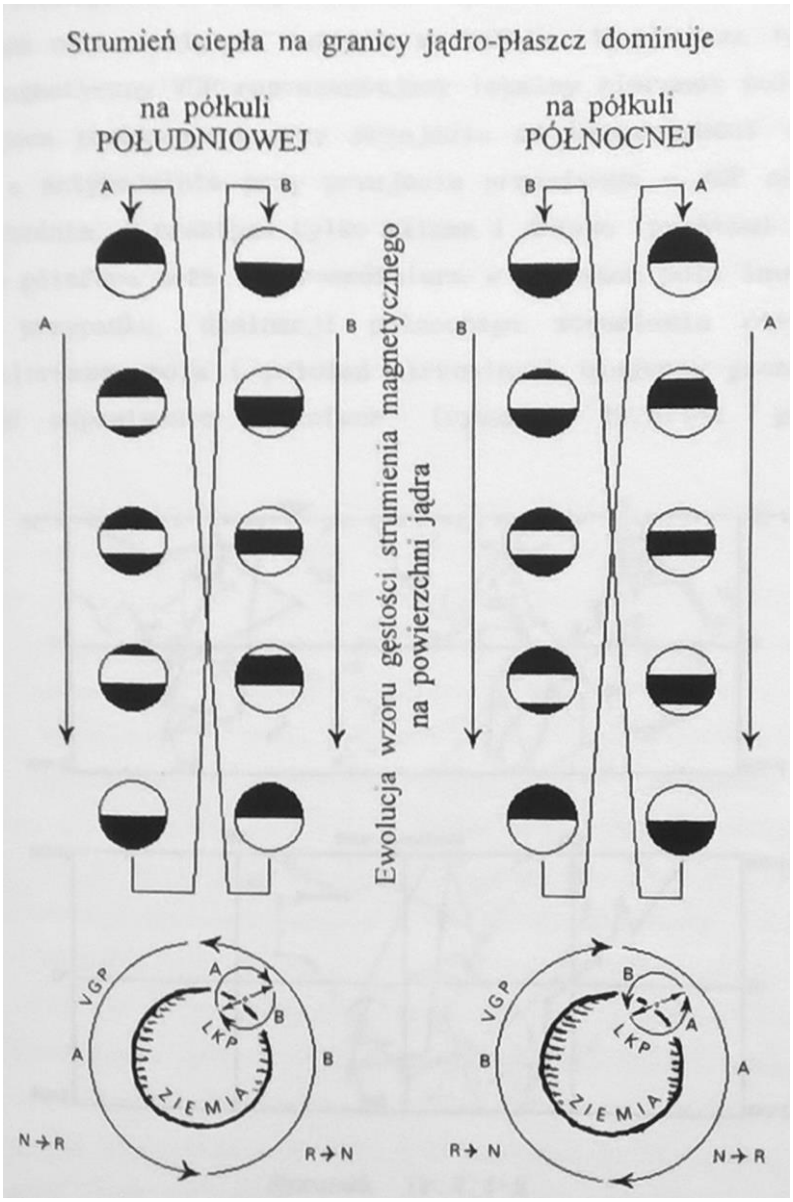

Figure 21. Scheme of changes sequence of the general (large-scale) magnetic flux distribution on the Earth core surface (CMB) during reversal in the two axially symmetric cases (breaking reflective N-S symmetry of the heat transfer to the mantle): domination of the Southern heat flux (left sequence) and domination of the Northern heat flux (right sequence). The dark areas on the Earth core surface represent positive magnetic flux (component $\boldsymbol{Z} > 0$; corresponding to *normal* dipole field configuration on the North hemisphere), and the bright areas represent negative magnetic flux (component $\boldsymbol{Z} < 0$; corresponding to *normal* dipole field configuration on the South hemisphere). Below, corresponding rotations of local field observed on the Earth's surface, and their respective rotations of the virtual magnetic pole (VGP) position representing the local field direction, were depicted for each sequence. Conventionally, the *normal* (N) position of VGP is the Northern one.

5.B) Research on the use of Ground Penetrating Radar in pavement diagnostics

The *Ground Penetrating Radar* (GPR) method belongs to the family of the geophysical measurement methods. It is based on the analysis of the electromagnetic wave transition through the investigated medium and it is directed on obtaining information about the structure and about some material properties of the medium, which are expressed through its electromagnetic characteristics (mainly permittivity and related quantities: wave velocity, absorption, conductivity). As a wave method, this technique is very closely related to seismic methods, having a lot of common terminology with this discipline in the area of data acquisition, processing and interpretation. Thus the GPR method is counted as the category named as *near-surface Geophysics*. Although, this method stems from geophysics and in geophysics has its methodological background, it seems that the widest area of its application is the diagnostics of constructions. The research described below concerns its applications in the road construction industry.

Diagnostics of the inter-layer boundary condition. The upper part of the bituminous pavement is in general, a package consisting of several layers made of stone-asphalt mixtures. This layered structure is usually very well visible on GPR echograms. Delamination i.e. lacking mechanical binding of two contacting layers is one of the specific defects of the package. Delaminations appear as a result of improper or total lack of gluing of the two layers during the package construction. The delamination below the uppermost layer leads to very fast destruction of the layer during intense exploitation of the road, while opinions as to the results of deeper delaminations are divided.

The several years research project was dedicated to assessment possibilities of the GPR technique in identification and investigation of delamination. These efforts covered tests of properties of the measuring system, laboratory simulation of the horizontal crevice for the GPR signal, numerical modelling of the generation of this specific signal, GPR measurements in the field (on roads sections, where such problems occurred) and control drillings. This seemingly simple task turned to be very difficult in practical realization, and the literature dedicated to this problem contains unambiguous and not very constructive opinions. The investigations of delaminations in the real field conditions is particularly difficult, because at the beginning they are invisible and one can get to know about them incidentally during control drills and the extent of the problem appearing is usually unknown. The laboratory simulation of the expected response of the widespread flat crevice for the GPR signal is also a large problem. The geometrical realms of the measuring system demands the model of the layer package to have the horizontal dimensions of value at least 2mx2m to avoid a generation of the scattered signal on the edges of the model plate. Otherwise this signal is early enough that it masks the head pocket of the analysed crevice respond. The horizontal crevice should also be distant from the upper and lower surface of the model plate of at least one wavelength. Indeed, after several months of efforts this simulation had came off (Sudyka et al. 2009, Sudyka and Krysiński 2011), but the most convincing illustration was provided by a simple analogue of the crevice having a form of a thin plate scanned directly without participation of the external medium in which the crevice is typically immersed (Sudyka and Krysiński 2011, Krysiński and Sudyka 2012). It turns out that the signal generated by such thin crevice, as a result of reverberation inside the crevice, has a form essentially different from the reference signal generated on the flat contact boundary surface of two media having a permittivity contrast. If the crevice is thin enough than the wavelength in the medium filling it, then the multiples are not observed as separate signals, but as a result of interference the resulting signal is similar to the time derivative of the reference signal (Sudyka and Krysiński 2011,

fig. 22). This specific signal shape corresponding to a thin crevice was named the *double reflection*, and this notion turns to be very useful in the echogram interpretation practice.

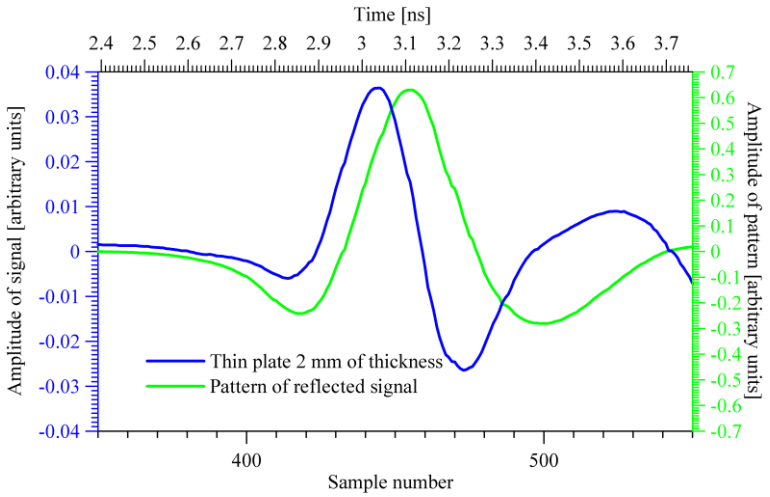

Figure 22. Comparison of a GPR signal reflected from a thin (1.9 mm) acrylic panel (*double reflection*; blue curve) and a signal reflected from sheet metal (*single reflection*; green curve).

Documenting the relation between the physical condition of the interlayer boundary and the shape and amplitude of the generated response signal turned out to be a much more difficult task than the preliminary investigations. The spectacular manifestations of the predicted phenomena (fig. 23) were found much later (Sudyka et al. 2011). The reliable description of such cases plays a very important rule in diagnostics, because it allows to make suppositions coming from echograms in situations with limited records available, e.g. when invasive verification is not possible.

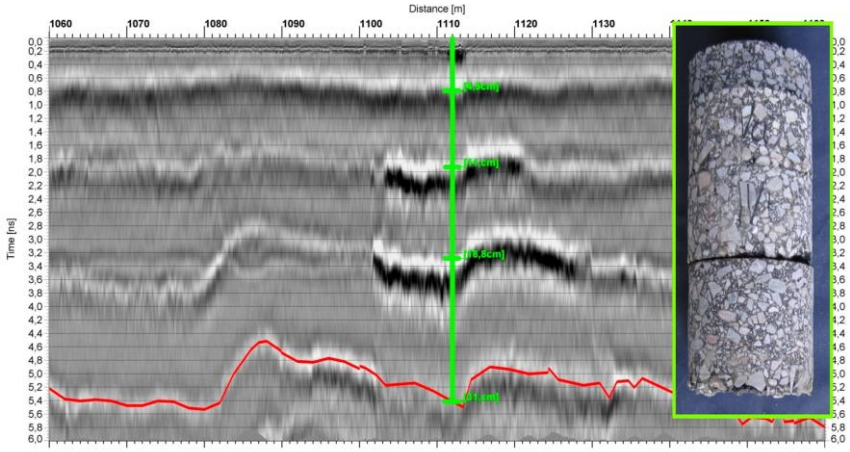

Figure 23. Example of the positive *double reflections* (2 and 3.4-ns depth) manifesting *wet delaminations* in a road where disastrous hydrological conditions occurred.

The results of the described research is of a diagnostic utility in the identification of delaminations, however it is not free from complications (Krysiński and Sudyka 2012). Not always the double reflection signifies an improper interlayer bonding. Its presence is an expression of a material difference occurring at the interlayer boundary, and expressed – to be more precise – in permittivity contrast, which has no obvious translation into mechanical properties. Too abundant binder (typically bitumen) applied during gluing (before the laying out the new layer) into the boundary can generate a strong negative double reflection identical

to the one associated with an empty (dry) open delamination crevice. On the other hand , even if the mechanical binding between layers was broken, this state has no GPR manifestation until the crevice is not open. Moreover, the weak double reflections are difficult to be spotted in the presence of the residual masking background (related to the internal antenna reverberation) in the analysed signal. The problem of diagnostic criterion looks completely different in case of strong positive double reflections, which manifest the presence of a high-permittivity material (compared with the vicinity) in the interlayer boundary lamina, that is to say, a material essentially foreign to the asphalt package (water, clay minerals, metal grains or fibres etc.). Then such a reflection is a strong finding signalling a very probable defect of binding. There are also situations, where the structural context provokes a generation of the delamination (like a rebar's level in concrete plates) giving an additional reason strengthening the supposition of delamination occurrence even if its GPR manifestation is weak. This methodology has already found some special applications, for instance in investigations of the mechanism of storage and transport of fluids in a unique seep deterioration process of the asphalt package. The knowledge about complications of the interlayer boundary structure and their manifestations in the GPR signal has also got a large significance in procedures of precise determination of the package layers thickness.

Diagnostics of the pavement cracks structure. The pavement cracks are a common type of the construction defect. They can be generated as a result of improper construction project's assumptions, or improper pavement building, but they can represent the road wear and tear resulting from exploitation. Being a well-visible manifestation of the deteriorating, the cracks are an object of a particular research interest. The goal of the several years' research project was the assessment of the GPR technique in the area of the cracks' structure diagnostics. In this problem an interesting paradox occurs: the well-visible cracks on the surface (sometimes several centimetres wide) not always have a noticeable response in the GPR image. But also reversed situations occur where the cracks hardly visible on the surface or even hidden below the uppermost layer give quite a clear response.

In the frame of laboratory investigations, the tests of the methods' horizontal resolution in distinguishing two objects (e.g. metallic bars) situated closely one to the other and at some distance from the antenna were performed to check the minimum width enabling the crack width assessment. One important model simulation was also performed: the scanning during a passage of the antenna over the edge of a vertical acrylic glass plate (in perpendicular direction), being a simplified model of a crack crevice (Krysiński and Sudyka 2013). This measurement turned out to be very significant on a practical level; despite of idealised form of crevice the weak response generated was at the limit of the system's sensitivity. It means that the real empty crevice of the width of several centimetres, immersed in the external medium is practically not possible to be observed through a GPR measurement, because of masking signal's presence: reflection from the upper surface of the medium, internal reverberation in the antenna and chaotic scattering signals generated on the medium granular structure. The preliminary laboratory measurements were also supported by numerical modelling.

The road pavement diagnostics has a special predilection for the transversal cracks of the pavement. In this case, one can polarise the electric field of the emitted signal of the *air-coupled* antenna in the direction parallel to the cracks (i.e. perpendicularly to the profile), that is in maximal scattering configuration, while simultaneously crossing the crack structures perpendicularly, which allows for the identification of the structure in the echogram. Then, with such setting, the scanning is possible by regular inclusion of the measuring vehicle into the ongoing traffic without any traffic reorganization and the measurement can be made on long distances. The scanning using the *ground-coupled* antenna is also possible. These antennas usually have significantly better capabilities in resolution and sensitivity, but for the

practical reasons mentioned the measurement is much more difficult and it can be performed only locally.

The field measurements focused on several road sections in current use, where the problems of cracking occurred. The central task was to precisely correlate the echograms with positions of the cracks observed visually on the surface. The task was not quite easy, because the standard localization methods used in the road investigation practice do not give a possibility of finding the visual observation position in the echogram with an uncertainty less than 50 cm. After the application of several methods of measurement and correlation of the entire position-sets of these methods it was possible to find the precise visual observation position of each crack on the echogram, where respective GPR manifestations are to be expected.

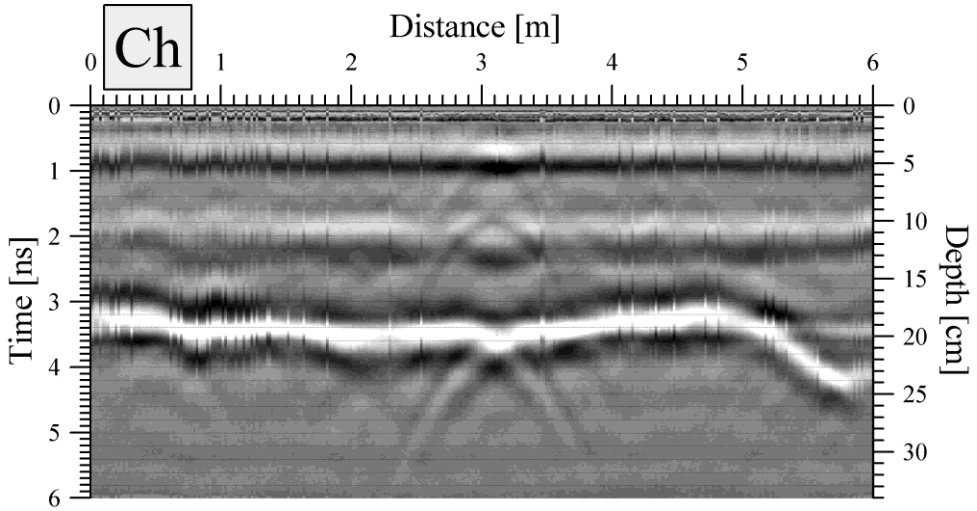

Figure 24. Example of the *Christmas tree pattern (Ch)* of GPR manifestations of a crack (Krysiński & Sudyka 2013), consisting of 4 hyperbolas (the crack is located at the distance 3.1 m).

The detailed review of the echograms allowed to build the list of characteristic cracks' GPR manifestations (fig. 24). The synchronous occurring of the elementary manifestations in the echogram (Krysiński i Sudyka 2013, 2016) has a particular significance during identification; both the simultaneous occurrence at different depths (suggesting common structural reasons) or on closely neighbouring profiles (signifying the lateral continuation of the structure; fig. 25).

The study of the typical GPR manifestations of the cracks has a phenomenological character, and it consisted of formation of a descriptive list thereof with some classification. The analysis of these scattering (diffractive) forms generated in the places where the cracks occur immediately opened extensive interpretation problems as to the geometry and material state of the structures responsible for the generation of the scattering signals. The places enriched by the particularly strong scattering ability have an accordance in depth with the interlayer horizons. Many of these forms have not got the shape of a typical scattering hyperbola corresponding to nearly point- or linear objects of small width. In opposition to, the form *chi* or form *V* suggest that the scattering structure has a considerable, at least decimetre wide lateral elongation (i.e. in the direction along the profile). Sometimes, this suggestion was in some opposition to an observation of a thin (sometimes millimetre) crevice at the surface, but it was in accordance to the laboratory simulations. Another family of questions concerned the material nature of the altered medium of the crevice, which obviously had a large contrast in relation to the surrounding medium. The attempt to recognize these problems with the use

of drillings made on selected and earlier scanned crack (Krysiński i Sudyka 2013) gave many significant statements (fig. 25).

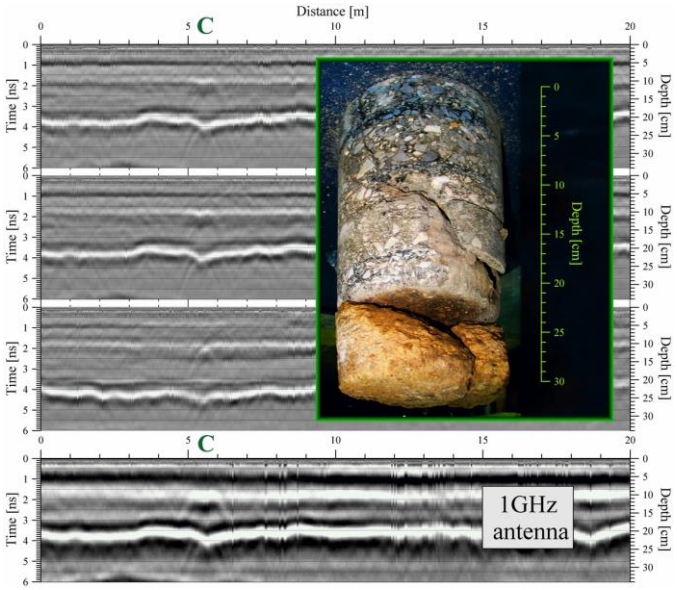

Figure 25. Echograms (from the top: left, central and right profile 2.2 GHz antenna and left profile 1 GHz antenna) and drilling core showing crack structure (crack located at distance 5.5 m), being responsible for generating strong hyperbolas (Krysiński & Sudyka 2013).

The crack structures generating the scattering of GPR-wave have really impressive dimensions. Frequently these are structures, which are well-developed (several centimetres thick or more) as a result of long lasting (many years, usually several ten of years) mechanical activity of the crevices in the asphalt package, hidden below a provisory overlay. In the sub-base below the crevice, severe material changes occur of more than decimetre thickness. These investigations allowed for the definition of an effective procedure of the transversal cracks' deep-rooting assessment. The procedure is directed in order to check whether the cracking process is deep-rooted in its form of extensive, earlier developed structures, demanding far-reaching technological interventions, if these interventions are expected to be successful.

6. REFERENCES

Becker J.J., Sandwell D.T., Smith W.H.F., Braud J., Binder B., Depner J., Fabre D., Factor J., Ingalls S., Kim S-H., Ladner R., Marks K., Nelson S., Pharaoh A., Sharman G., Trimmer R., von Rosenbürg J., Wallace G. & Wetherall P., 2009. *Global bathymetry and elevation data at 30 arc seconds resolution: SRTM30_plus*. Mar. Geodesy, 32, 355-371.

Bielik M., Grabowska T., Bojdys G., Csicsay K., Šefara J. & Speváková E. 2006. *Density modelling of the lithospheric structure along the CELEBRATION 2000 seismic profile CEL01*. Contr. Geophys. Geod. 35, 81–97.

Czuba W., Grad M., Luosto U., Motuza G., Nasedkin V. & POLONAISE P5 Working Group 2001. *Crustal structure of the East-European Craton along the POLONAISE'97 P5 profile*. Acta Geophys. Pol. 49 (2), 145–168.

Grabowska T., Bojdys G. & Dolnicki J., 1998. *Three-dimensional density model of the Earth's crust and the upper mantle for the area of Poland*. J. Geodynamics, 25 (1), 5-24.

Grabowska T., Bojdys G., Bielik M. & Csicsay K., 2011. *Density and magnetic models of the lithosphere along CELEBRATION 2000, profile CEL 01*. Acta Geophysica 59 (3), 526 – 560.

Grad M., Tiira T. & ESC Working Group, 2009. *The Moho depth map of the European Plate*. Geophys. J. Int., 176, 279-292, DOI: 10.1111/j.1365-246X.2008.03919.x.

Guterch A., Grad M., Materzok R. & Perchuć E., 1986. *Deep structure of the Earth's crust in the contact zone of the Palaeozoic and Precambrian Platforms in Poland (Tornquist-Teisseyre Zone)*. Tectonophysics, 128, 251-279.

Guterch A., Luosto U., Grad M., Yliniemi J., Gaczyński E., Korhonen H., Janik T., Lindblom P., Materzok R. & Perchuć E., 1991. *Seismic studies of crustal structure in the Teisseyre-Tornquist zone in northwestern Poland (preliminary report)*. Publs. Inst. Geophys. Pol. Acad. Sc. A-19 (236), 147-156.

Guterch A., Grad M., Keller G.R., Posgay K., Vozár J., Spičak A., Brueckl E., Hajnal Z., Thybo H. & Selvi O., 2000. *CELEBRATION 2000: Huge Seismic Experiment in Central Europe*. Geol. Carpath. 51(6), 413–414.

Krysiński, L., 1992. *On the mathematical connections of planetary rotational deformations with Love's tidal problem*. Phys. Earth planet. Inter., 72(3-4), 137-152, doi: 10.1016/0031-9201(92)90198-5.

Krysiński L., 1996. *Pochodzenie pola magnetycznego Ziemi - historia badań i obecny stan poglądów*. Przegląd Geofizyczny, 41 (3), 193-218.

Krysiński L., 1997. *Morfologia dynamiczna pola magnetycznego Ziemi w świetle jego ewolucji w okresie 1990-1995 i ogółu wyników paleomagnetycznych*. Rozprawa doktorska, Uniwersytet Warszawski, Wydział Fizyki, Instytut Geofizyki, Warszawa.

Krysiński L., 2006. *Comparative, Velocity-Dependent Gravity Modeling of the Density Section Along Three Carpathian DSS Profoles*. Geolines, Vol 20, 78-79 [4th Meeting of the Central European Tectonic Studies Group, Zakopane, Poland, April 2006].

Krysiński L. & Sudyka J, 2012. *Typology of reflections in the assessment of the interlayer bonding condition of the bituminous pavement by the use of an impulse high-frequency ground-penetrating radar*. Nondestructive Testing and Evaluation, 27 (3), 219-227, doi: 10.1080/10589759.2012.674525.

Krysiński L. & Sudyka J. 2013. *GPR abilities in investigation of the pavement transversal cracks*. J. App. Geophys. 97, 27–36.

Krysiński L. & Sudyka J., 2016. *Case Study of Step-frequency Radar Application in Evaluation of Complex Pavement Structure*. Transportation Research Procedia, 14, 2930-2935, ISSN 2352-1465, http://dx.doi.org/10.1016/j.trpro.2016.05.412.

Krysiński L., Grad M. & Wybraniec S., 2009. *2D gravity modelling as a method of searching for deep-seated horizontal density contrasts in the Earth's crust*. Geophysical Research Abstracts, 11, EGU2009 3141, EGU General Assembly 2009, Vienna.

Pabisiak E., 2005. *Analiza zgodności przekroju głębokich sondowań sejsmicznych z polem grawitacyjnym wzdłuż profile P4*. praca magisterska. Uniwersytet Warszawski, Wydział Fizyki, Instytut Geofizyki, Zakład Fizyki Litosfery.

Puziewicz J., Czechowski L., Krysiński L., Majorowicz J., Matusiak-Małek M., Wróblewska M., 2012. *Lithosphere thermal structure at the eastern margin of the Bohemian Massif: a case petrological and geophysical study of the Niedźwiedź amphibolite massif (SW Poland)*. Int J Earth Sci (Geol Rundsch) 101, 1211–1228, DOI 10.1007/s00531-011-0714-7.

Pavlis N.K., Holmes S.A., Kenyon S.C. & Factor J.K., 2008. *An Earth Gravitational Model to degree 2160: EGM2008*. Geophys. Res. Abs., 10, EGU2008-A-01891.

Sudyka J. & Krysiński L., 2011. *Radar Technique Application in Structural Analysis and Identification of Interlayer Bounding*. International Journal of Pavement Research and

Technology, ISSN 1996-6814, May, vol. 4, nb. 3, Published By: Chinese Society of Pavement Engineering, 176-184.

Sudyka J., Krysiński L. & Harasim P., 2009. *Sprawozdanie z realizacji pracy pt.: „Analiza możliwości wykorzystania techniki radarowej w ocenie stanu połączeń międzywarstwowych"; sprawozdnie częściowe, etap II – zadania 3-5*. Instytut Badawczy Dróg I Mostów, Zakład Diagnostyki Nawierzchni, Warszawa.

Sudyka J., Krysiński L., Jaskuła P., Mechowski T. & Harasim P., 2011. *Radar technique in application of interlayer identification connections*. 5th International Conference 'Bituminous Mixtures and Pavements', Thessaloniki, 1-3 June, 2011, 1449-1459.

Środa P., Czuba W., Grad M., Guterch A., Tokarski A.K., Janik T., Rauch M., Keller G.R., Hegedűs, E., Vozár J. & CELEBRATION 2000Working Group (2006). *Crustal and upper mantle structure of the Western Carpathians from CELEBRATION 2000 profiles CEL01 and CEL04: Seismic models and geological implications*. Geophys. J. Int. 167, 737–760. doi:10.1111/j.1365-246X.2006.03310.x.

Turcotte D.L. & Harris R.A., 1984. *Relationship between the oceanic geoid and the structure of the oceanic lithosphere*. Mar. Geophys. Res., 7, 177-190.

Wybraniec S., 1999. *Transformations and visualization of potential field data*. Polish Geological Institute, Special Papers 1, 88 pp.

Lech Krysiński